UNIVERSITY OF
EASTERN FINLAND

MOLECULAR DYNAMICS STUDY OF IRON-RICH CLAY

Fayoyiwa Aderemi Deborah

Master's thesis

Department of Chemistry

Physical Chemistry

583/2017

TABLE OF CONTENT

ABSTRACT

Smectites have high swelling ability, which makes them excellent candidates for use as buffers in repositories for the disposal of high-level radioactive waste. Many factors that affect the swelling process of smectites have to be considered and justified before they can be used in these repositories. One of such factors was considered in this study.

In this we study, we looked at the effect iron has on the swelling pressure of smectites using montmorillonite and beidellite as our smectite samples of study. Iron is a component of sealing materials used in the construction of underground repositories for high-level nuclear waste disposal and it is important to know how iron affects the swelling behavior of smectite buffers used in these repositories.

Four clay models (two beidellite and two montmorillonite models) were used in this study. For each clay model Fe^{3+} was substituted for Al^{3+} in the octahedral layer gradually until the maximum level of substitution was reached. The swelling pressures of the clay models (without Fe and with varying percentage of Fe-content) in bulk water solution was modeled with Molecular Dynamics simulation method using the spring model as studied by Sun et al (2015).

The effect of iron was more pronounced in the montmorillonite models than in the beidellite models studied. Swelling pressure decreases with increase in iron content. The major effect was seen at low Fe-content, at about 25% Fe-content and at high dry density.

This study gives important information on the effect of iron on the swelling pressure of smectites. This information can be used as a guide to screen smectites intended for use as engineering barriers in repositories for high-level radioactive waste disposal and other suitable industrial and engineering applications.

CHAPTER 1: INTRODUCTION

Composition and structure of clay minerals are key determinants of their physicochemical properties, therefore, clay minerals that appear to have the same structures might be very different in terms of chemical composition. [1] Crystal structures and small particle size of clay minerals are responsible for some of their unique properties like catalytic abilities, low permeability, cation exchange capabilities, swelling behavior and plastic behavior when wet. [2]

Clays are aluminosilicates that are hydrated and they contain other minerals, fine-grained clay minerals and metal oxides. [3] Clay minerals are a group of hydrated aluminosilicates that are dominant in the clay-sized (less than 2 µm) fraction of soils. [4] Clay can be defined to a large extent, based on its composition, the purpose for which it is meant and also its particle size. Figure 1 shows an image of sodium montmorillonite clay as viewed under electron microscope.

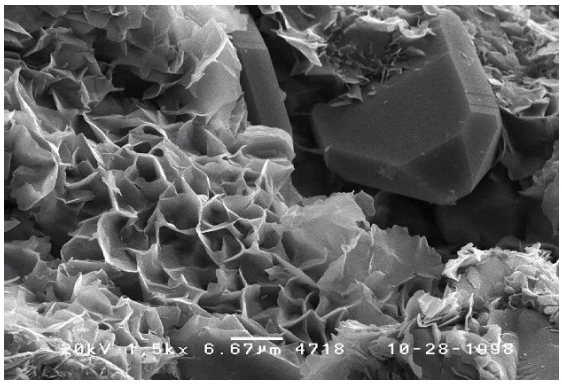

Figure 1. Bentonite clay [5]

Uses of clay boils down to its physicochemical properties which contribute well to its end product. Because of their physical properties, kaolins are used for paper coating and bentonites in drilling mud. Kaolins are also used to make fiberglass because of their chemical properties. [1] Clays are used to for making pharmaceutical products, they are used as catalysts in many industries, clays are used to purify oils, and they are also used in ceramic industries to make bricks, china wares and porcelains. Clay minerals with great ability to swell and also have suitable cation-exchange capabilities, low permeability and long term structural stability are used as clay barriers for nuclear and chemical waste disposal. [2]

New frontier is being broken to ensure safe disposal of nuclear waste by burying them deep underground. Nuclear waste disposal in underground disposal systems have been researched in time past and there are several on-going researches in some countries like Finland, Sweden, Canada and Japan. Clay serves as sealants in the vessels or canisters of underground nuclear waste disposal systems. Due to the unstable nature of Fe (ability of undergo reduction or oxidation), there is hesitation in the use of iron-rich clay as sealants in underground repositories for nuclear waste disposal.

Swelling pressure refers to the pressure that is expected to hold clay minerals at constant volume when the conditions of the environment are likely to cause increase in volume of the

clay minerals. [6] The swelling process of clay is determined by several factors like the type of cations in the interlayer, the location and quantity of layer charge which is as a result of isomorphic substitution in the clay layers, and also the component of the clay minerals. [7]

For clay to work effectively as a sealant in the nuclear waste disposal system, the right type of clay must be used and also the swelling pressure of such clay must be determined.

Different families of clay minerals, smectites, properties of clay, iron-rich clay as well as computational simulation of clay will be discussed in subsequent chapters.

CHAPTER 2: CLAY MINERALS

Clay minerals can be primary or secondary. Primary minerals are formed from igneous or metamorphic rocks at high temperatures and pressures, example of primary mineral is kaolin. Secondary minerals like smectites are formed from less resistant primary minerals through breakdown and weathering. These weathered and broken-down minerals are referred to as phyllosilicates. This is because they are leaf-like and they exhibit platy or flaky habit. [5] Examples of clay minerals are Kaolin, Smectite, Illite, Chlorite, and Palygorskite- Sepioloite minerals.

Clay minerals fall into either the 1:1 or 2:1 structure. The 1:1 type of clay minerals have an octahedral layer and a tetrahedral layer of clay on top of each other, while the 2:1 type of clay minerals have an octahedral layer situated in the middle of two opposing tetrahedral layers. [8]

To join octahedral and tetrahedral sheets in 1:1 structure, one hydroxyl in the octahedral layer is replaced by an oxygen in the apical position of tetrahedral sheet. For joining the layers in 2:1 structure, oxygen at the apex in tetrahedral sheet takes the place of 2/3 of hydroxyls present in the octahedral layer positioned between two tetrahedral sheets. [5] Figures 2 below shows diagrammatic representation of 1:1 and 2:1 structures of clay minerals as recorded by

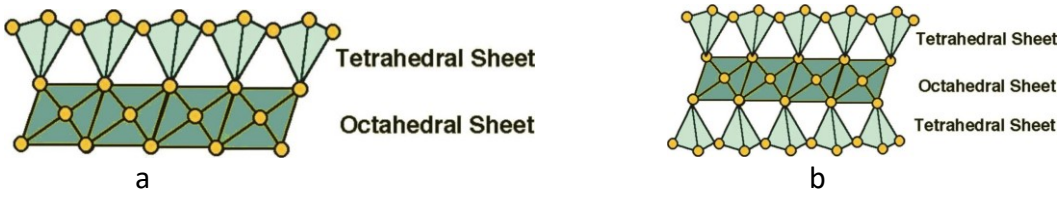

Figure 2. 1:1 (a) and 2:1 (b) clay structures [5]

Clay minerals have similar chemical composition, layered structure and affinity for water (extent of water intake depends on the type of clay). [9] Classification of clay minerals by Al-Ani and Sarapää (2008) is illustrated in Figure 3.

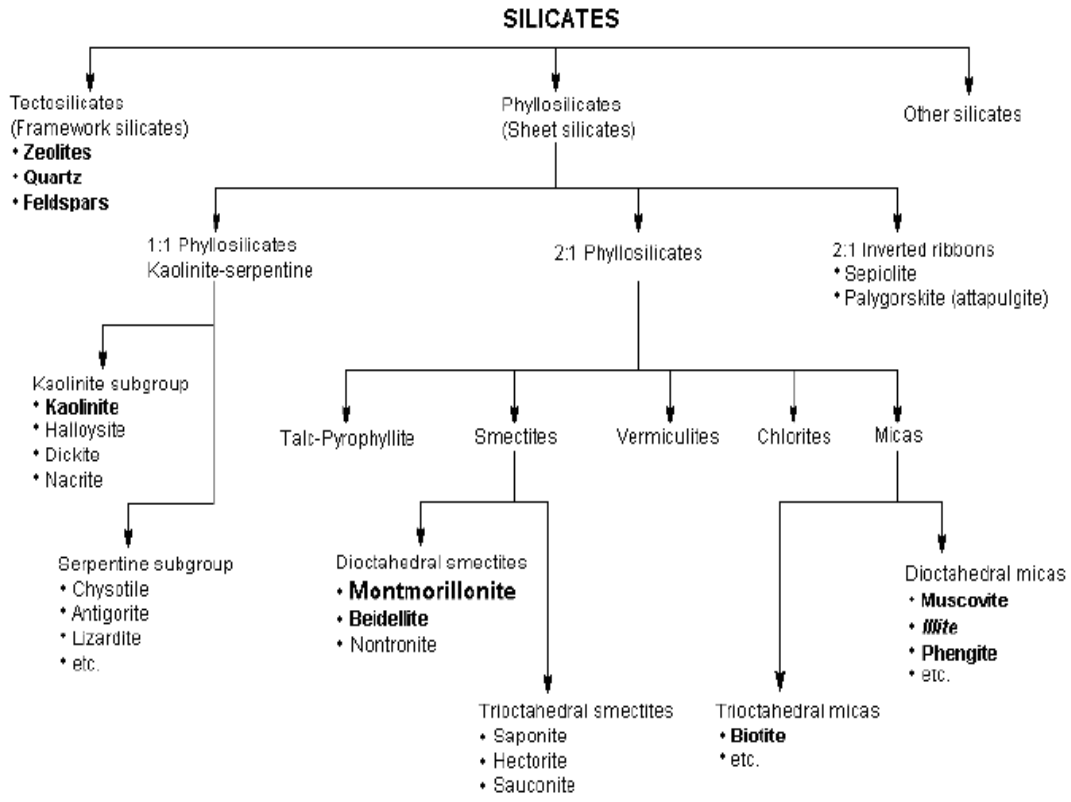

Figure 3. Classification of clay minerals [5]

There are two layers associated with clay minerals; the octahedral and tetrahedral layers. In the octahedral layer, when bonded to OH^- or O^{2-} anions , Mg^{2+}, Fe^{2+}, Fe^{3+} or Al^{3+} cations shows six-fold coordination. The cation is located in the center of the resultant structure. These structures are attached to each other by sharing their six tips. This implies that for trioctahedral clay layer, one anion is attached to three cations and for dioctahedral clay layer, the anion is attached to two cations leaving a site vacant. [10] Octahedral sheets in dioctahedral smectites are dominantly occupied by trivalent cations while in trioctahedral smectites the octahedral sheets are dominantly occupied by divalent cations. [8] In the octahedral layer, hydroxyls and oxygens are found very close to each other, also magnesium, aluminum and iron atoms are found in octahedral coordination. [1] Figure 4 is a diagrammatic representation of the octahedral and tetrahedral clay layers.

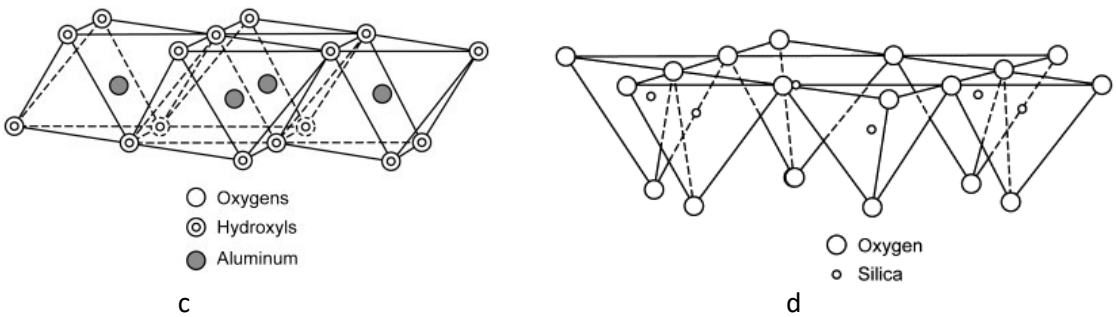

c d

Figure 4. Octahedral (c) and tetrahedral (d) clay layers [1]

Common cations found in the tetrahedral sheets are Si^{4+}, Fe^{3+} and Al^{3+}. [8] The tetrahedral sheets are composed of SiO_4^{4-} or AlO_4^{5-} which are connected by sharing three tips out of four tips; one oxygen is found at the peak and the other three oxygens are basal. [10] In the tetrahedral sheet, the silicon atom is located at equal distance from the four oxygens or hydroxyls (which are possible) arranged in a tetrahedron form, the silicon atom is located at the middle of the strcture as represented in Figure 4 above. [1]

In both tetrahedral and octahedral layers, isomorphic substitution takes place which results in permanent charge. When Al^{3+} replaces Si^{4+}, and Mg^{2+} is present in place of Al^{3+} in tetrahedral and octahedral layers respectively, a negative layer charge equal to one electron is produced. [11] Clay layers can also have neutral electrical charge when the cation substitution in tetrahedral layer has a sum of +4 as is found in Si^{4+} or when trivalent cation like Fe^{3+} replaces Al^{3+} in the octahedral layer. [8]

Magnitude of layer charge can be explained with substitution in pyrophillite $[(Si_8)(Al_4)O_{20}(OH)_4(0H_2)_2]$. A layer charge of -0.5 will be obtained if the cation in tetrahedral layer is substituted with a cation of lower valence; $(Si_{7.5}Al_{0.5})(Al_4)O_{20}(OH)_4(0H_2)_2$. $(Al^{3+})_{0.5}$ replaced $(Si^{4+})_{0.5}$, therefore a negative charge of $(1)_{0.5}$ is obtained. A neutral charge can be obtained if a trivalent cation (Fe^{3+}) replaces Al^{3+} in the octahedral layer,$(Si_8)(Al_{3.5}Fe_{0.5})O_{20}(OH)_4(0H_2)_2$. The net charge in the octahedral layer after the substitution is zero.

The space between the sheets contains water and weakly bound cations, the cations are responsible for the balance of the overall negative charge displayed by the silicate-aluminate sandwich unit. [9]

Cations occupy smaller space in tetrahedral sheet than in octahedral sheet. This implies that smaller sized cations like Si^{4+} occur in the tetrahedral sheet and larger sized cations such as Mg^{2+} and Fe^{2+} occur in octahedral sheet. Cations with sizes between the tetrahedral and octahedral layers can occur in either layer as seen in the case of Al^{3+}. [12]

Layer charge is a very essential parameter of clay minerals used to determine clay properties that are important for industrial applications. One of such properties is the shrinking and swelling of clay minerals. [13] Layer charge is very instrumental to the classification of 2:1 type of clay minerals. [14]

CHAPTER 3: SMECTITE AND BENTONITE BUFFER

Smectites are phyllosilicates with 2:1 structure, they have total negative charge ranging from 0.2 to 0.6 in half unit cell. Examples of smectite minerals are montmorillonites with dominant elements like Ca-montmorillonite, Na-montmorillonite, Li-rich montmorillonite (hectorite), Mg-rich montmorillonite (saponite), Fe-rich montmorillonite (nontronite), and Al-rich montmorillonite (beidellite). Smectite is made up of 66.7% SiO_2, 28.3% $Al2O_3$ and 5% H_20. [5]

Substitution takes place in smectites. Considerable substitution occurs in the octahedral layer but not so much substitution happens in the tetrahedral layer. [15] Smectite clay structure as illustrated by Haydn H. Murray can be seen in Figure 5.

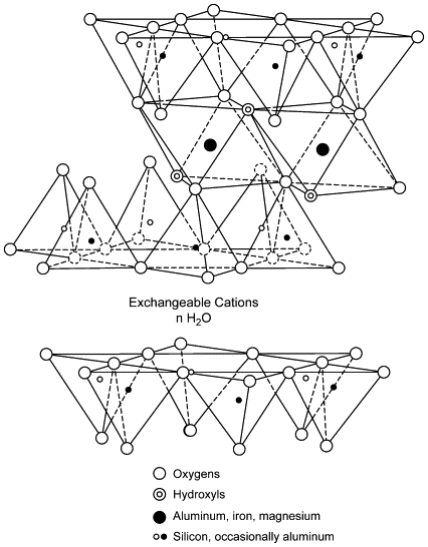

Figure 5. Structure of smectite clay [1]

Bentonites are clays which are made of montmorillonite mineral crystals which are mostly arranged in stacks of unit layers. [16] Bentonites have various uses some of which are; bonding materials in foundries, pet litter especially cat, binding agents in production of iron ore, removal of impurities in oil, buffers in underground waste disposal system or repositories for high level nuclear waste (HLNW).

Bentonites are expansive clays that swell significantly with water intake. Montmorillonite is responsible for the expansive property of bentonites. [17]

In addition to Na- and Ca-montmorillonite, the bentonite buffer material also contains small amount of other minerals like zeolites, quartz, pyrite, feldspars, gypsum/anhydrite and calcite/siderite. [18]

Swelling pressure occurs when montmorillonite rich clay takes up water and expand in a confined environment. The bentonite buffer is confined and restricted by the surrounding rocks in the repository and the volumetric expansion is also limited. [18]

The physical stability of the bentonite buffer can often be characterized by balancing the interactions of clay particles and drag force of the groundwater flow. Interactions of clay particles can be used to determine the chemical stability of bentonite buffer. [18]

CHAPTER 4: PROPERTIES OF CLAY

Among the many properties of clay minerals, solubility, cation exchange capacity, plasticity, hydraulic conductivity, permeability, catalytic abilities and thixotropy are discussed in this chapter. The latter part of the chapter focuses on swelling and swelling pressure of clay.

Swelling: Swelling is a key property of clay minerals that qualifies them as a good candidate for High Level Nuclear Waste (HLNW) disposal. When the activities of solid phase and liquid phase of clay minerals are put together, they cause swelling. Swelling involves volume increment of soil due to the effect of different type of solutions, swelling is dependent upon particle size, percentage of clay composition, mineralogical composition, type of fluid in the soil, type of cations that are exchangeable, percentage of carbonates and organic matter, extent of unsaturation amongst other factors. [19] Increase in lamellar spacing of clay minerals also contributes to swelling of the clay mineral, a less compacted clay mineral swell more than a compacted clay mineral. [20]

The mineral content of clay minerals has high importance on the swelling ability of the clay mineral. Swelling of clay minerals increases with increase in the mobility of the lattice or structure of the clay minerals. Kaolites have rigid structure which is responsible for their little swelling ability because they interact with water to a minimum extent. Smectites on the other hand have mobile structures and they swell to large extents. [19]

Adsorption: Adsorption occurs when molecules of one substance adheres to the surface of another substance. Adsorptive property of clay is due to the negatively charged clay surface. The negative electrostatic charge of clays attract cations from the soil solution, these cations can be retained or attached to the surface of clay mineral. Adsorption property of clay results to cation exchange of the clay minerals.

Water adsorption in expansive clay is caused by hydration, capillarity and osmosis. Out of these three mechanisms, hydration and osmosis play important roles in the clay swelling process. [21]

Clay minerals can be used to purify oils, for color removal treatments and can also be used to remove toxins because of their adsorptive properties. Bentonite can be used to adsorb any kind of radiation. [22] Synthetic talc, Sepiolite and kaolin are good dye/color removers. Sepiolite was investigated for its ability to remove brilliant green dye and synthetic talc was studied for the ability to remove acid orange 7 as well as reactive red 3. [23] Clay minerals also adsorb water to their surfaces. The ability of clay mineral to adsorb water is linked to its CEC per unit area. [24]

Cation Exchange Capacity: Clay minerals to a large extent can attract and hold cations due to their chemical structures although there is variance depending on the type of clay minerals. A part of the many properties of clay minerals is that they have ability to absorb some ions and hold them in a state where they can be easily exchanged. Exchangeable ions are located on the outward surfaces of the clay mineral (except for smectites) and the exchange reaction has no effect on the structure. Cations that are often exchanged in clay minerals are Na^+, K^+, NH_4^+, H^+, Mg^{2+} and Ca^{2+}. [15] According to Grim, cation exchange takes place when bonds are

broken close to the crystal edges, as a result of lattice substitution and hydrogen of open surface hydroxyls which is exchangeable.

Cation exchange capacity (CEC) can be obtained by dividing the quantity of excess cation retained by mass of the sample. Variable charge as well as permanent charge are included in CEC, measuring CEC for pure smectites is easier compared to smectite samples with some other components. [25]

High charge on lattices of clay minerals (e.g Na-montmorillonite) gives them the ability to change water in the interlayer and associated cations with organic molecules which are more polar, such as ethylene glycol, quaternary amine and poly-alcohols. This property is of essence because it can be transformed into organoclays which are great products with a lot of uses. [1]

Plasticity: Plasticity is the property of clay that exhibits changes in shape without breakage or crack when a mixture of clay sample and water is acted on by an external force. Upon the reduction (to a value that corresponds to yield stress) or complete removal of the external force, the shape of clay sample is maintained. [26]

Major factors that influence clay's plasticity are connected to physical properties of the clay, especially water characteristics (surface tension, viscosity), specific surface area of particle size distribution, clay mineral type and dispersion state of particles which are dependent on the proportion and nature of additives as well as the ionic change capacity. [24]

Permeability: Permeability is another essential property of clay minerals. It is the property or capacity of clay minerals to transmit fluid without impairment of the medium. It shows the ease with which fluids flow in the presence of unequal pressure. [27] Permeability and hydraulic conductivity of clay are very similar properties. Hydraulic conductivity is a major factor that affects the performance of clay as sealants in waste disposal system for high-level nuclear waste. [28] Expansive clays like smectites possess low permeability. Water doesn't pass freely through such clay minerals; they retain water which in one way contributes to their swelling.

Permeability depends on the grain size of the clay particles (density) and the quantity of cracks the clay sample has. The smaller the grains that make up the clay sample, the less permeable the clay sample is. Clay particles possess large surface area where hygroscopic water binds to leading to more difficulty in the movement of fluid. [29]

Catalytic abilities: Clay minerals can be used as parts of materials for making catalysts. Bentonites especially are very useful for catalysis. [30] Bentonites are utilized in some industrial processes like polymerization and dimerization of unsaturated carbons and also for phenol alkylation. [31] By adjusting clay's surface area and acidity using acid activation, catalysts can be formed. [32]

Protons replace exchangeable cations when acid activation is taking place. Acid sites are formed in clay structures when the replaced exchangeable cations and a fraction of cations in the octahedral layer dissolve. 2:1 layer type of clay minerals are often used to prepare catalyst because they possess high acidity and large surface area in comparison to the 1:1 layer type. [33]

Transition metals whose lattices contain kaolinites due to acid activation and calcination show high selectivity for benzene alkylation using benzyl chloride and catalytic activities. [34] Aluminum and iron fortified montmorillonites show excellent catalytic activity in benzylation reaction. [35] Another use of clay catalysis is the purification of essential oil, glyceride oil as well as petroleum oil, clay catalysis is also employed in general organic synthesis and pyrolysis. [26]

Thixotropy: Thixotropy is the ability of clay minerals to form gels upon standing and to become liquid when stirred or disturbed. Thixotropy contributes to ability of clay minerals like Na-montmorillonite and hectorite to be used as suspending agents. Na-montmorillonite is the first material used as drilling mud and hectorite is used in high quality paint and also used in pharmaceutical and medicinal suspensions. [1]

Thixotropy shows the time it takes to move from one microstructure state to the other, it could be between several states of flow to rest or from rest. Microstructural flow change is due to breakdown (because flow stresses) and buildup (based on Brownian motion and inflow collisions) competing. Buildup takes much longer time than breakdown. [36]

Swelling of clay

All clay minerals swell but the extent to which they swell differs. Smectites and vermiculite clay minerals swell to very large extent while swelling of clay minerals like chlorite, kaolin, illite and pyrophyllite is very minimal (almost inexistent).

Most expansive clay contain smectite or vermiculite clay minerals. The interlayer of these minerals are expandable and in their natural states, they have large specific surface areas, which produces forces of unsatisfied water adsorption. [37]

The swelling property of smectites contribute to their relevance to many environmental and industrial processes. Ability of smectites to be used as engineered barriers in nuclear waste repositories is due to their swelling ability, also the swelling ability of smectites is not favorable in oil and gas production. [7]

Swelling in smectites occurs when exchangeable cations are hydrated and this leads to expansion. [38] In smectite samples, there are interlayer cations which readily adsorb surrounding water, due to negative layer charge, smectite minerals easily swell with the influx of water into the interlayer. [7]

Smectite minerals are used as backfill materials and buffer in underground disposal systems for high level nuclear waste placed several hundred meters below ground level. The buffer material creates a low permeable zone around the repository's canister because nuclear wastes should be disposed of far away from human and animal contacts. Self-sealing ability is the ability of smectites to make a better zone that cannot be penetrated when around these dangerous nuclear wastes. [39]

During water saturation, the aggregates in the compact bentonite expand and after a prolonged period of time, the large (and small) inter-aggregate pores are partially or fully occupied by clay gel the expanding aggregates produces. This expansion of aggregates gives

rise to swelling pressure. Degree of expansion of bentonites used as buffer in repositories is small because they are confined in space. [18]

Swelling process of clay

There are two known swelling processes in expansive clay minerals, these processes are known as crystalline swelling and osmotic swelling. Crystalline swelling takes place when the water content is low which is mainly as a result of initial hydration of exchangeable ions in the interlayer. Crystalline swelling happens when water goes into the interlayer like successive molecular layers sequence which leads to the interlayer being separated in a stepwise manner for about three layers of water. On the other hand, osmotic swelling happens at high water content and shown as continuous separation of the interlayer which results from the movement of water to the mineral interlayer because of the differences in concentration of ion within bulk pore water and interlayer. In osmotic swelling, interlayer separation proceeds beyond the four water layers known with crystalline swelling and this leads to partial or total disassociation of the interlayers and the formation of a hydrated solid state. [40]

Factors affecting swelling of clay

There a lot of factors that affect the swelling properties of clay minerals. These factors can be broadly grouped into two; environmental and structural variables. The environmental variables consist of humidity, external pressure, temperature as well as osmotic pressure. The structural variables include layer charge, charge location and interlayer cation.[7]

For expansive clay like samples like MX-80, montmorillonite is responsible for the swelling of smectites. Montmorillonite minerals contain exchangeable cations and interlayer water between their layers. Absorption of water into the interlayers of the clay minerals causes montmorillonites to expand. [39] Stepwise swelling behavior of montmorillonite indicates that interlayer cation is of great importance to the swelling of clay. [7]

Interlayer expansion process can be explained to occur in two different stages. In the first stage, oxygen surfaces are separated while cations in the interlayer are still attached to the surfaces. For the second stage, by interaction with the water molecules, cations are detached from the oxygen surfaces. [24]

When expansion is related to humidity or vapor pressure at which it takes place, the effect of the interlayer cation becomes apparent. [24] From the work of Barshad, Isaac, he studied clay samples, which are saturated with cations of different sizes but equal charge, the relative humidity at which expansion occurs increases with increase in ionic radius. It is important to mention that the rate of hydration in the beginning of expansion is almost the same for all ion sizes. Also for clay samples with cations of varying charges but equal radius, relative humidity at which expansion occurs reduces with increase in charge (rate of hydration when expansion began is almost the same is for all of the ions). Lastly, he also observed clay samples, which are saturated with the similar cation, but different quantity and he noted that increase in the number of cations causes reduction in the relative humidity wherein expansion occurs and here also, rate of hydration is about equal for the different montmorillonite.

From the observations above, the relationship between expansion and relative humidity in clay is important because it offers a possible way to evaluate the forces of attraction of the interlayer that binds the separate lattice layers. [41]

Smectite minerals with divalent cations expand more at lower water content than smectite minerals with monovalent cations, Na-montmorillonite forms three-layer hydrate at higher water content. [42]

Swelling pressure

For the understanding of swelling process of expansive clay, analysis of swelling pressure is of utmost importance. [6] Swelling pressure results from expansive clay with restricted volume. Swelling pressure is the highest amount of stress applied on expansive clay minerals bombarded with water to maintain a constant volume. Swelling pressure is seen as variation in osmotic pressure between central plane in-between two particles and equilibrium bulk solution. [44]

When making designs of structures that involve swelling of clay in a restricted environment (like underground repository for high-level nuclear waste), swelling pressure is an indispensable parameter. Swelling pressure must be justified for the intended purpose to prevent great damage to structures and rigid supports that work in close contact with expansive clay minerals. [45]

CHAPTER 5: IRON-RICH CLAY

Occurrence of iron-rich clay

Iron-rich smectites can be found in soils. [46] and sediments, many different conditions are responsible for the formation of iron-rich clay. These many conditions can be generally classified into three major categories namely hydrothermal alteration, fresh crystallization/precipitation and chemical weathering in no particular order. For chemical weathering, parent rocks, soil materials and sediments that are not or marine origin are altered by reactions which take place because of different climatic conditions. In this process, iron-rich smectites are obtained as intermediate products. Previous work by Nahon, 1982 [47] recorded huge amounts of iron containing smectites as the intermediate phase of the weathering process of pyroxene and olivine to primary oxides from extensive study of lateric weathering.

Iron-rich saponites are result of hydrothermal alteration. They occur extensively in marine environments, at low pressures and temperatures (less than 500 bars and less than 150^0C), diabases and oceanic basalts react with supersaturated seawater. [48]

In addition to hydrothermal alteration and chemical weathering, direct crystallization has been recorded to lead to formation of ferruginous smectites. In the work of Isphording (1975)[49], in the presence of elevated temperature water and siliceous fluids that contains

iron, a nontronite was formed from the solution as a result of crystallization in Venezuelan Guayana. A picture of iron-rich clay is shown in Figure 6.

Figure 6. Iron-rich clay [50]

Nontronite

Nontronite is a smectite clay mineral that occurs as the iron-rich member of the dioctahedral sub-group of montmorillonite-beidellite-nontronite series. [49] Nontronite is an octahedral montmorillonite in which iron is predominant. [51] All smectites contain structural iron but smectites that contain above 0.3 iron per $[O_{10}(OH)_2]$ are referred to as iron-rich smectites or iron-rich montmorillonite. [52]

Layer charge in nontronites is high and they result from isomorphic substitution in smectite clay minerals. Nontronites are formed naturally in oceanic sediments. [53] From previous studies, it was observed that iron being present as trace element in smectite's crystal structure has huge influence on its physicochemical properties which in turn influences agriculture, environment or industrial processes in which smectites are involved. [54] An image of notronite clay mineral is shown in Figure 7.

Figure 7. Nontronite [55]

There are other iron-containing smectites apart from nontronites such as saponite, ferrosaponite, volkonskoite and yakhontovite.

Iron in smectites

In the smectite structure, iron can be located in both the tetrahedral and octahedral layers. Iron (III) exits in either the tetrahedral layer or octahedral layer [14], while iron (II) can only be found in the octahedral sheet. Dioctahedral smectites most times contain very little amount

of iron (II), but trioctahedral smectites are likely to contain large amount of iron (II) and iron (III) also. [56]

Some smectite minerals exist in nature with different amounts of Fe (II) in the octahedral layer, but normally, the Fe (II) readily oxidizes to Fe (III) which leads to decrease in layer charge when the smectite mineral is in contact with water vapor and air. [57] According to Stucki (1988)[56], layer charge does not lead to cation exchange capacity at all times due to some counter ions that can be non-exchangeable because of layer collapse.

Series of studies have been carried out on how the in situ changes of the oxidation state of Fe affects the layer charge of dioctahedral smectites. Initial reports by Roth et al. (1968, 1969) [58,59]showed that the reduction of Fe (III) in the octahedral layer to Fe (II) did not affect the cation exchange capacity. In subsequent studies in which the atmosphere around the reduced clay was contained in a way that oxidation is prevented, an increase in both cation exchange capacity [60] and layer charge [61] was observed as Fe (III) was reduced to Fe (II) in the octahedral layer.

Oxidation of trioctahedral smectite containing Fe (II) is a natural occurrence and this can be an important factor which causes dioctahedral Fe (III) smectites to be formed. [62]

Reduction of smectites that contain Fe (III) takes place in sediments and soil when conditions that causes reduction (like flooding) are introduced [56], microbial activity can also be responsible for the reduction. [63] These processes to a large extent affect the physicochemical properties of clay minerals especially the swelling ability and cation exchange capacity, which affects the clay structure and permeability. By controlling the oxidation state, some properties of Fe-containing clay minerals may be modified in situ. [56]

Iron substitution in smectites

Clay properties and behavior change when Fe is being substituted for other ions in smectites. The properties of iron can change in situ and this ability makes iron unique among other elements found in clay minerals. [56]

Tetrahedral substitution, lower valence octahedral substitution or octahedral vacancies substitution are responsible for the layer charge in trioctahedral smectites. Fe (III) ions present in octahedral layer reduces the negative charge. This may be due to oxidation of Fe (II) saponite. [56]

Effect of iron substitution in smectites

Cation exchange capacity and Layer charge are majorly affected by iron substitution in smectites. For smectites that are dioctahedral, layer charge is generated as a result of isomorphous substitution of ions with lower valency for aluminum in octahedral sheet or silicon in tetrahedral sheet. The effect of Fe can be seen in smectites when there is Fe (III) substitution in the tetrahedral layer or Fe (II) substitution in the octahedral layer. [56]

Another major property affected by Fe substitution in smectite is swelling ability of the smectite. Stucki (1988)[56] recorded a generic reduction in the swelling volume as replacement of Al in octahedral layer by other ions (Fe (III) inclusive) rises in the unit cell. According to the

observation of Chen et al. (1979) [64], tactoid size of Ca-Montmorillonite particles rises as octahedral Fe (III) content rises. In his work, Foster (1953) observed a lower swelling pressure in the more reduced fraction of the bentonite sample than the more oxidized sample.

The extent to which smectite layers are soluble in HCl has a direct relationship with the octahedral Mg and Fe substitution for Al. [56] Chemical reduction of Fe leads to obvious irregularities which causes Fe to dissolve [61] or structural O-H loss. [65]

CHAPTER 6: EXPERIMENTAL AND COMPUTATIONAL STUDIES OF CLAY

6.1 EXPERIMENTAL STUDIES OF CLAY

Different experimental techniques can be used to investigate the physicochemical properties of swelling clay. The techniques can be used either for the measurement of macroscopic properties (like water content and bulk volume) or for the measurement of microscopic properties (like spacing between interlayers). [66] Some of these techniques are discussed below.

X-ray diffraction: This technique is used for monitoring the d-spacing of clay layers. Clay mineral's swelling profile can be checked using X-ray diffraction (XRD) by sampling the clay minerals as the water content or relative humidity rises. [42] From previous studies, XRD involves measuring interlayer spacing of montmorillonites when different electrolytes are present and at different states of hydration. [67] Albeit being used for the measurement of the interlayer spacing, the usefulness of XRD has limitations, as it gives no straight information concerning interlayer species arrangement or how the interlayer species relate with clay layers.

Volume measurement: The extent of swelling of clay minerals and other swelling data are obtainable by measuring increase in volume when they clay sample is hydrated. Swelling index can also be gotten from this method. [66] From the work of Besq et al. (2003) after hydrating, some portion (2g) of sixteen commercial bentonites with distilled water for four hours, 20-42cm^3 volume was recorded. Chistidis et al (2006) used a related method but he added a calculated amount of sodium carbonate in order to obtain maximal swelling. Swelling indices was recorded at about 98-257, usage of swellmeter aided the continuity of linear expansion measurement of compressed calcium montmorillonite.

Thermo-gravimetric analysis: This method is capable of revealing water distribution in clay minerals across different determined locations with the structure, when clay minerals are hydrated, this method sheds more light on the swelling behavior of clay minerals. [68] One serious problem associated with using this method is the fact that fugacity of water greatly affects the main temperature recorded when it is being lost from the mineral. [69]

Bulk hardness test: The method has a close similarity to clay dispersion test, it is used to check swelling and hydration of clay particles. Bulk hardness is defined as a function of displacement and torque. Based on how hydrated the bulk is, there might be an increment in the torque

while extrusion is going on or it might get to a plateau area. When cuttings are not hydrated enough, they appear hard and they correspond to high torque value. [66]

There are few methods that can be used for estimation of layer charge, they are dependent on the connection amid layer charge, and the rest of the parameters associated with clay minerals. Cation exchange capacity (CEC) is one method for characterizing layer charge. [70]

Layer charge can be calculated from the structural formulae using the presented stoichiometric coefficients. Data from elemental analysis gives the structural formulae and they show how elements are distributed in the clay. [71]

Fixed-volume test method: This method is one of the several experimental methods for the determination of swelling pressure of clay samples. In this method, compacted clay samples are put inside a fixed-volume cell of a known diameter (shown in Figure 8). It is possible for direct contact to exist between the clay samples, porous frits and piston while in some cases, there is not direct contact. [72]

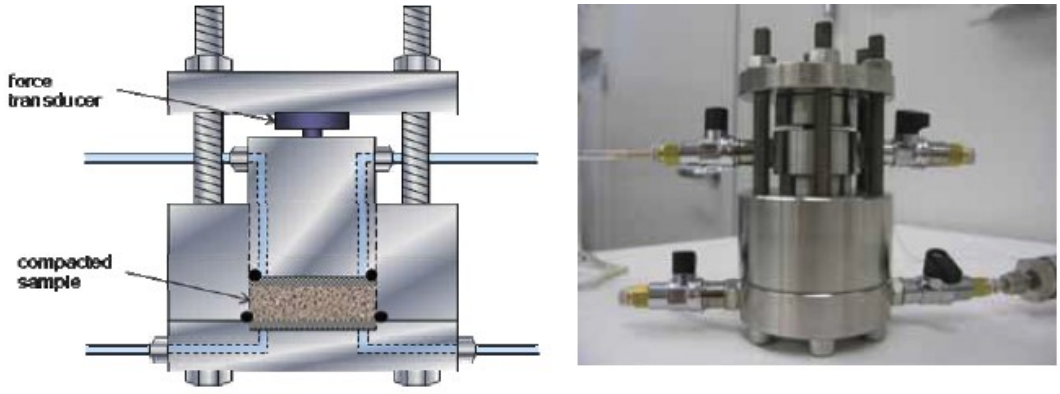

a b

Figure 8. Fixed volume cell; (a) schematic illustration and (b) photographic image [72]

A force transducer is put in place between the top plate and piston to enable the measurement of axial force due to swelling of the clay sample or internal pressure. The force transducer loads are recorded every thirty minutes using data logger. The clay sample is flooded with saturating solution with the help of peristaltic pump. Using the peristaltic pump, the solution flows slowly through the bottom circuit of the cell first for seven days and after that, the solution flows from the top and bottom of the cells for another seven to fourteen days. The bottom-up method of saturation allows air in the clay sample to go out from the top of the cell. [72]

Swelling pressure of the clay sample can be calculated from the axial force recorded using the relationship below. [86]

$$P_s = \frac{F}{A}$$

P_s is the swelling pressure, F is the axial force and A is the piston/clay sample contact area.

6.2 COMPUTATIONAL STUDIES OF CLAY

The use of computer simulation has created so much important impact in modern science which shows great growth in the use of computers across all fields of science. For about two decades now, the use of computer simulation in all field of science have being so effective that results from computational methods can stand with experimental and theoretical methods in value. [74] There are several methods of computational methods, the mostly used computational methods are discussed below.

Quantum Chemistry

Principle

Quantum chemistry is very important for atomic and molecular studies and also to model complex systems like the ones evolving in materials science and biology. It is based on solving electronic Schrodinger equation with computational tools, which calculates electron density, electronic energy and other properties when provided with the total number of electrons and the location of a group of atomic nuclei in the system, using a clearly stated approximation. [75]

Two highly productive approaches are available for solving electronic Schrodinger equation. There is approach based on wavefunction which expands electronic wavefunction as a sum total of optimized coefficients, orbitals and slater determinants. The simplest method of the wavefunction-based approach is the Hartree-Fock theory. Other types include second-order Moller Plesset perturbation theory;MP2, Complete Active Space with second-order Perturbation Theory; CASPT2 and Coupled Cluster with Single, Double and Triple perturbative excitation; CCSD(T).[75]

The basis of the other approach is Density Functional Theory (DFT) and it gives expression of total energy of a system as a function of the electron density. [76] For computational implementation, DFT is more attractive than Hartree-Fock Theory. [75]

Applications

For gaseous and aqueous small molecules, quantum chemistry calculations give relatively accurate results, these calculations are often used to verify experimental studies. Properties like structures, thermochemistry, different type of spectroscopic quantities and responses to external perturbations can be computed.[77]

There has been great increase in the materials-science application of quantum chemistry calculations in the last decade, now, highly complex chemistries and structures are being explored. For solids, computation of surface and bulk properties yields great agreement with experiment in many cases. [78] DFT methods have been successfully used to address optical properties and bandgaps of solids. [79]

Quantum chemistry calculations give many details, which are not gotten from experiments, and there is also a level of confidence in the outcome of quantum chemistry calculations that are not found in other empirical approaches. [75]

Monte Carlo (MC) Method

Principle

Monte Carlo method is one of the two major methods employed to simulate swelling in clay minerals. This method is based on classical statistical mechanics. Monte Carlo method can be used to check a material for infinite number of available configurations. [80]

A system's potential energy surface is looked into by checking various configurations gotten by putting random changes on a system according following previously defined rules. For a configuration, if the potential energy is not as high as the energy of the former configuration, then it is accepted, but if the energy is higher, it is only admissible with a probability weighted by Boltzmann factor. In MC method, properties are expressed as the mean value of the accepted properties. [66] MC simulation deals with the concept of water-water, clay-water, counter-ion-water and counter-ion-clay interactions. [81]

Applications

MC simulation method is highly effective when used to calculate thermodynamic averages of a system and it looks into a bunch of low energy configurations to locate global energy minimum in less timeframe compared to Molecular Dynamics simulation for a certain set of computational study. MC simulations is capable of giving averaged sets of low energy configurations of system which may be juxtaposed with XRD data or quasi-elastic neutron scattering (QENS) gotten from experiment. MC methods are highly instrumental for simulation of clay minerals swelling. [66]

MC methods can be used to carry out two major types of studies. For the first type of study, every MC step has small displacement of one of the atoms during the simulation, and quantum mechanical or empirical methods are used to compute the energy change. The second type of study involves the use of different types of variables and a model Hamiltonian. A very good model is the spin model in which every site has a variable which can be mapped on a vector that has interactions between neighbors being described by a model Hamiltonian. [74]

An example of MC simulation on clay is 'Monte Carlo Simulation of Interlayer Molecular structure in Swelling Clay Minerals. 2. Monolayer Hydrates' by Skiper et al., 1995. Figure 9 below is a representation of a system from Mc simulation.[82]

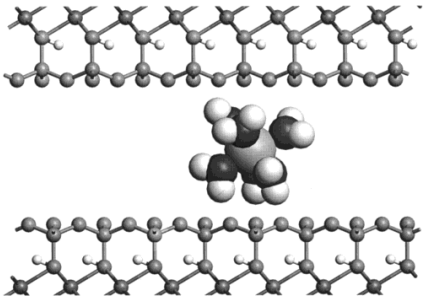

Figure 9. Equilibrium MC snap shot of Mg-beidellite in the z,x plane [82]

Molecular Dynamics (MD) method

Principle

MD method is suitable for investigating the equilibrium structure and longtime dynamics of complex systems. For MD simulations, interatomic interactions are seen as long-rage coulomb interactions and short-range van der Waals interactions. [82]

MD method incorporates temperature and anhamonic terms into simulation. The MD method exploits the basis that forces are linked to acceleration by Newton's equation of motion. The method starts with a big configuration of atoms and uses quantum mechanical or empirical method to calculate the force on every atom. This force is then changed to acceleration, with the use of algorithm for numerical time step, acceleration can be joined to the information of the previous and current positions of the atoms, velocities or accelerations to infer the location of every atom after a little period of time. The result of MD simulation portrays emergence of the positions and velocities of atoms in a system through time. [74]

Time steps correlate with about $1/20^{th}$ of the smallest natural period of vibration [74], the time step for MD simulations should be small and is mostly set to 1fs . It is also a possibility to simulate systems that have millions of atoms with empirical models by using modern algorithms which scale linearly with the number of atoms with large multi-processor computers having low latency inter processor communications [74].

A method that employs the use of MD and Ab initio simulations was developed by Car and Parinello in 1985 to solve coupling time propagation of nuclei in motion with determination of electronic structure. This method uses equation of motion to solve coefficients that are approximately in line with variational minimum orbital coefficients that can be gotten from a Density Functional Theory solution of electronic structure in every stage. The coefficients together with the nuclear positions evolve in sync. This method can reproduce accurately electronic structure's time evolution with the time-evolution of the nuclear positions if the fictitious coefficient masses are correctly picked.

Some force fields suitable for clay mineral simulation are Universal force field (UFF), Teppen force field and ClayFF force field. In recent times, MD simulations involving clay minerals uses the new developed CLAYFF force field by Cygan et al. (2004). This CLAYFF force field differentiates an element into different types based on its structural position (tetrahedral or octahedral sheet and the neighboring elements) and gives van der Waals parameters and partial charges to every type of atom. It defines a bond-stretch parameter for the structural OH and an angle bend parameter for the octahedral metal and OH. [83] The interlayer water parameters in the CLAYFF force field are from Simple Point Charge (SPC) water model. [84]

Applications

MD method of simulation can be used to show evolution of systems with temperature and pressure for equilibrium phenomena and evolution of systems with time for systems in which the sample is reacting to a particular disturbance. MD simulation can also be used to compute distribution functions like distribution of orientation of molecules or of the locations of atoms. MD simulation can be used for analysis of dynamics, often by using time-correlation functions.

In the case of fluids or highly-dynamic systems simulation, calculation of diffusion constants from the analysis of single atom motions is possible. For simulation of solids, detailed information on the time scales for dynamic processes can be gotten from studies of fluctuations through time-correlation functions. [74] Figure 10 shows a representation of a system using MD simulation.[83]

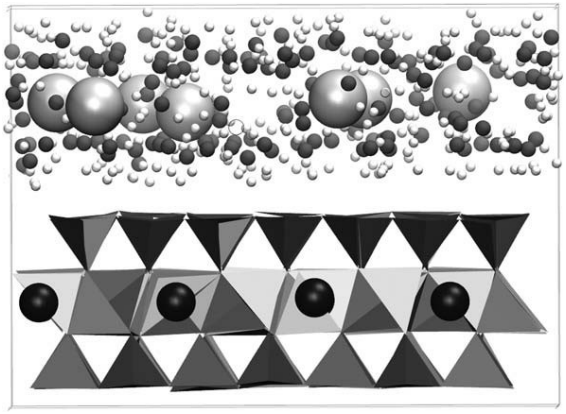

Figure 10. A snapshot of the MD simulation box [83]

Running quantum chemistry calculation is very expensive and this is one of the major reasons why quantum chemistry calculations are by passed for other simulation methods. Also, unlike other empirical and semi-empirical methods, approximations and assumptions on the basis of physical principles of the system are made. To an extent, this assumptions and approximations reduces the level of confidence one has in results gotten from quantum chemistry calculations.

Statistical error can be found in MC simulations as well especially if the steps are short, running enough steps is recommended in order to reduce these errors and how they affect analysis.

Owing to the discussions above and juxtaposition of all three considered simulation methods, swelling of clay minerals is best studied with a combination of MC and MD simulations. In Table 1, some computational studies on iron-rich clay are presented.

Table 1. Some computational clay studies

REFERENCE	METHOD	MODEL	RESULT
Alexandrov et al.[85]	DFT	Nontronite [$Fe_2Si_4O_{10}(OH)_2$]	The most favorable edge face is FeO(H) and mixed FeO(H)-SiO(H) is the least.
Alexandrov et al.[86]	DFT	Nontronite [$Fe_2Si_4O_{10}(OH)_2$]	a. The main factors that affect the rate of electron transfer are structure and nature of the closest neighbor local environment and the extent of covalency of bonds between ligands mediating electron hops and iron b. Higher reorganization energy and weaker electronic coupling present in Fe-rich clay minerals causes electron mobilities that are lower compared to iron oxides.
Geatches et al. [87]	DFT	a. Ideal nontronite (smectite with all-Fe^{3+} octahedral and Al^{3+} tetrahedral substitution) b. Garfield Nontronite;NG (smectite with Fe3+ and Mg2+ substitution for Al3+ in octahedral sheet, and Al3+ in the tetrahedral sheet) c. NG-1 (Smectite with only Fe3+ in octahedral sheet and around 20% substitution in tetrahedral sheet)	Reduction occurs to the highest degree in iron present in the octahedral sheet while oxidation occur to the highest extent in iron of the tetrahedral sheet.

CHAPTER 7: STUDY AIM

The study is carried out to find out the swelling properties of iron-rich clay in bulk solution using molecular dynamics simulation. The study aims to check how these properties affect the use of iron-rich clay as a sealant in underground disposal systems for high level radioactive waste. The study also aims at investigating the extent to which iron-rich clay can be used as sealants in underground repositories, because of the unstable nature of iron.

CHAPTER 8**:** METHOD AND MODELS

8.1 **General introduction to MD simulation in clay modelling**

MD simulation of clay imitates the actual relationship of clay with its surroundings. Using MD for simulation, the bulk system can be adjusted to accommodate up to thousands of atoms. The conditions for simulation can be adjusted as well. MD simulation can be used to investigate the thermodynamic and kinetic properties of clay.

8.2 **Clay sample**

Sun et al. [88] studied the effect of layer charge and charge location on the swelling pressure of dioctahedral smectites. It was observed that decrease in layer charge increases the swelling pressure of dioctahedral smectites and for a fixed layer charge, increase in percentage charge in the octahedral layer causes increase in the swelling pressure. Figure 11 shows a summary of this study, swelling pressures were obtained at 1650kg/m^3, 1200kg/m^3 and 990kg/m^3. From figure 11, the effect of layer charge and charge location is prominent in structures A, C, H and J. This informs our choice of structures for this study.

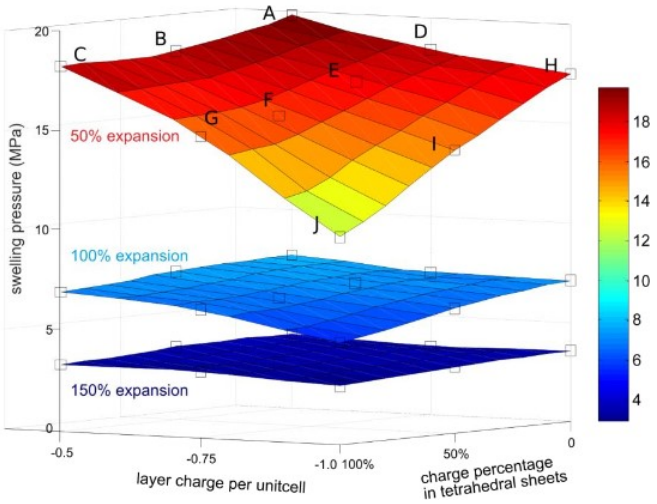

Figure 11. Swelling pressure as a function of layer charge and charge percentage in tetrahedral sheets.[88]

For this study, four dioctahedral smectites structures were studied. Iron content in each structure was increased gradually until the substitution limit was reached. Structures A, C and J have 25%, 50%, 75% and 87.5% Fe-content but structure H has 25%, 50% and 75% Fe-content because 75% Fe-content is the maximum that is achievable in structure H. Al^{3+} in the octahedral sheet was substituted with Fe^{3+}. Choice of Fe^{3+} over Fe^{2+} is due to the lack of Fe^{2+} in the CLAYFF force field used. Also, from the experimental data obtained, the effect of Fe^{2+} on swelling pressure of smectites is significantly low compared to Fe^{3+}. As shown in Table 2 below, the structures studied have different layer charges and locations (octahedral and tetrahedral sheets).

Table 2. Information on clay structures studied

STRUCTURE	MOLECULAR FORMULA (4 UNIT CELLS)	LAYER CHARGE	% CHARGE IN TETRAHEDRAL SHEET
A	$Si_{32}(Al_{14}Mg_2)O_{80}(OH)_{16}(0H_2)_8$	-0.50	0%
C	$(Si_{30}Al_2)(Al_{16})O_{80}(OH)_{16}(0H_2)_8$	-0.50	100%
H	$Si_{32}(Al_{12}Mg_4)O_{80}(OH)_{16}(0H_2)_8$	-1.00	0%
J	$(Si_{28}Al_4)(Al_{16})O_{80}(OH)_{16}(0H_2)_8$	-1.00	100%

Structures A and H are montmorillonite clay models while structures C and J are beidellite clay models. All four clay structures studied have the 2:1 clay structures, which has one tetrahedral layer sandwiched between two octahedral layers. Each clay sample studied has two clay layers directly on top of each other. The distance between the beginning of the first layer and the beginning of the second layer is referred to as d-spacing. For each clay sample, there were seven different d-spacings (14Å, 15Å, 16Å, 18Å, 20Å, 25Å and 30Å). In structures A and C, each clay layer contained four sodium ions (Na^+) while each clay layer in structures H and J contained eight sodium ions (Na^+) to balance the charges.

Strip substitution method was used to insert iron atoms into the clay structure. In this method, placement of iron atoms at the clay edges was avoided as much as possible and all atom substitution was made so that they are related by inversion symmetry. Also, iron substitutions were made to have similar arrangement patterns. Figures 12(a)-12(d) show the octahedral sheet (8 unit cells) of all structures studied (obtained from VMD) with their atom placements having 25% Fe-content.

Color code for models in Figures 12-15

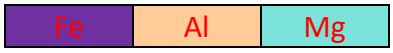

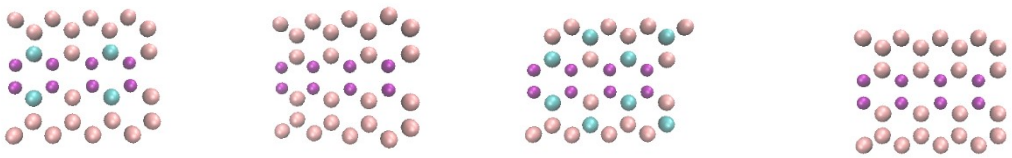

(a) (b) (c) (d)

Figure 12. Clay structures (a) A , (b) C , (c) H , (d) J with 25% Fe-content

Figures 13(a)-13(d), 14(a)-14(d) and 15(a)-15(c) show the octahedral sheet (8 unit cells) of the clay sample obtained from VMD with their atom placements with 50%, 75% and 87.5% Fe-content respectively.

(a) (b) (c) (d)

Figure 13. Clay structures (a) A , (b) C , (c) H , (d) J with 50% Fe-content

(a) (b) (c) (d)

Figure 14. Clay structures (a) A , (b) C , (c) H , (d) J with 75% Fe-content

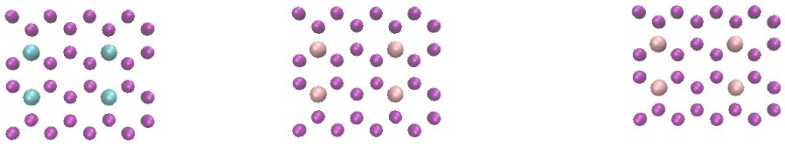

(a) (b) (c)

Figure 15. Clay structures (a) A , (b) C , (c) J with 87.5% Fe-content

8.3 **Construction of simulation system**

Clay models were put in a box of the same dimensions for all simulation. Water molecules was added to the simulation box in the simulation process. All structures with varying Fe-content and at different d-spacings have slightly different number of water molecules in the simulation box. For all simulations carried out, there were a little above six thousand water molecules for each.

8.4 **Computational details**

Molecular Dynamics (MD) computational method was used with CLAYFF force field and GROMACS package (version 5.1.4) as the MD model. The computational simulation started with Energy minimization (EM) which prepares the clay samples for further simulation and is then followed by the equilibration simulation with NPT lasting 10ns. The isobaric-isothermal ensemble (NPT) was set at 1 bar and 300k and data was collected at 0.1ps intervals with both clay layers at fixed positions. After EM and NPT simulation, convergence of the total energy, temperature and pressure was confirmed before moving to NVT simulation. With the help of Visual Molecular Dynamics (VMD), a molecular visualization program, it was also confirmed that there was no shift in the clay layer positions during NPT simulation. Figure 16 shows images taken from VMD.

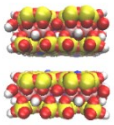

Fig. 16a. Isolated clay structure

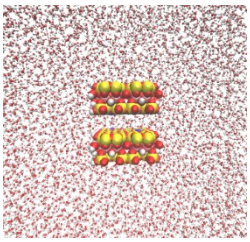

Fig. 16b. Clay structure in bulk water solution

Swelling pressure simulation was carried out using the NVT ensemble with 50ns simulation time, although only the last 40ns was used for swelling pressure analysis. For the canonical ensemble (NVT), 0.5fs time step was used and data was collected at 5ps intervals. Force constants were introduced to limit the movement of the upper clay layer. For every clay sample studied, force constants ranging from 1 to 10 was employed for each d-spacing.

8.5 **Swelling pressure measurement**

The swelling pressure of the clay samples was monitored by using the spring model as studied by Sun et al., 2015. [89] In this model, the bottom clay layer was held at a completely fixed position in x, y and z directions. The upper layer was only restrained in the x and y directions (it could move in the z direction). A mechanical spring at equilibrium was fixed to the upper clay layer; this mechanical spring possesses force constant and obeys Hooke's law.

When the clay sample starts to swell, displacement in the z-direction of the upper clay layer from its initial position (before swelling) leads to the compression of the spring from its equilibrium position and also causes increase in the spring force which restrains the movement of the upper layer. The spring model is illustrated in Figure 17 below.

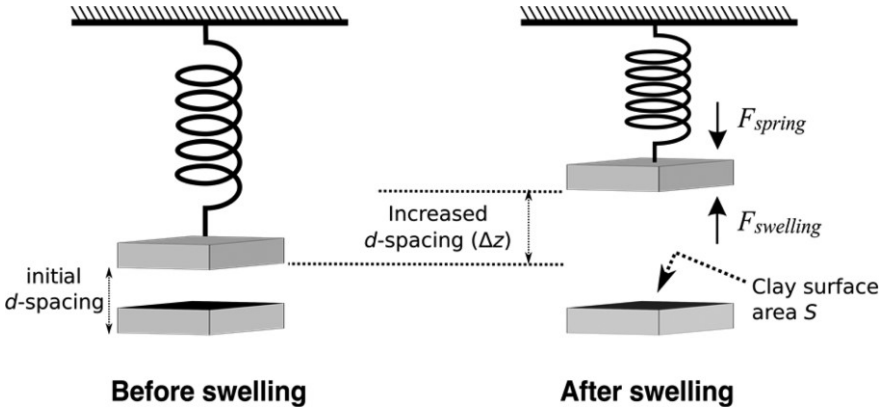

Fig. 17 Illustration of the spring model [89]

The change in the d-spacing of the clay sample corresponds to the change in the spring length. At equilibrium state in the clay swelling, the force of on the spring is taken to be equal to the force of clay swelling. Deformation of the spring only occurs in the z-direction (because the upper clay layer was restrained in x and y- directions), and from the deformation of the spring the swelling force and swelling pressure can be calculated as shown below.

$$P = \frac{F(swelling)}{S} = \frac{F(spring)}{S} = \frac{k\ x\ \Delta z}{S}$$

Where P = swelling pressure, F(swelling) = swelling force, F (spring) = force on spring, Δz = change in d-spacing, S = clay surface area and k = force constant. [89]

CHAPTER 9: RESULTS AND DISCUSSION

9.1 **Swelling pressure**

In all clay structures studied, swelling was observed in all iron-rich smectite samples, especially in the lower d-spacing of samples (1.4, 1.5, 1.6 and 1.8nm). A general decline in swelling pressure with increase in d-spacing was observed for all clay samples studied. The clay swell due to sodium ions in the interlayer, which attract water molecules to the interlayer from bulk solution. [88] In the same clay structure, samples with different percentage of iron contents have almost the same swelling pressure.

Structures A, C, J and H without (0%) Fe-content has the highest swelling pressures. Structure A has the highest swelling pressure of all four structures studied while structure J has the lowest swelling pressure. The extent of the swelling pressure of structures C and J is fluctuates between structures A and J, but in most cases structure H has higher swelling pressure than structure C. Change in swelling pressure (ΔP) for all structure with Fe-content was obtained by subtracting their values from corresponding values in similar structure without Fe-content.

9.1.1 **Clay structure A - $Si_{32}(Al_{14}Mg_2)O_{80}(OH)_{16}(0H_2)_8$**

Structure A has -0.50 layer charge with 0% charge in the tetrahedral sheet. Figure 18(a) shows the decreasing trend in the swelling pressure of structure A (at varying Fe-content) with increase in swelling pressure. Power function was used for the fitting shown in Figure 18(a), Table 3 compares power and exponential functions for the graph shown in figure 18(a) and they are almost the same. Fittings obtained from the graph of structure A are very good.

Structure A has the highest swelling pressure of all studied structures and in most cases, the swelling pressure decreases with increase in Fe-content as shown in Table 4. Table 4 shows the d-spacings at 1500, 1200 and 900 kg/m^3 with their corresponding swelling pressures. ΔP is the difference in swelling pressures of structures with Fe-content and structures without Fe-content. The swelling pressures of structures with Fe-content was subtracted from the swelling pressures without Fe-content at the same dry density value.

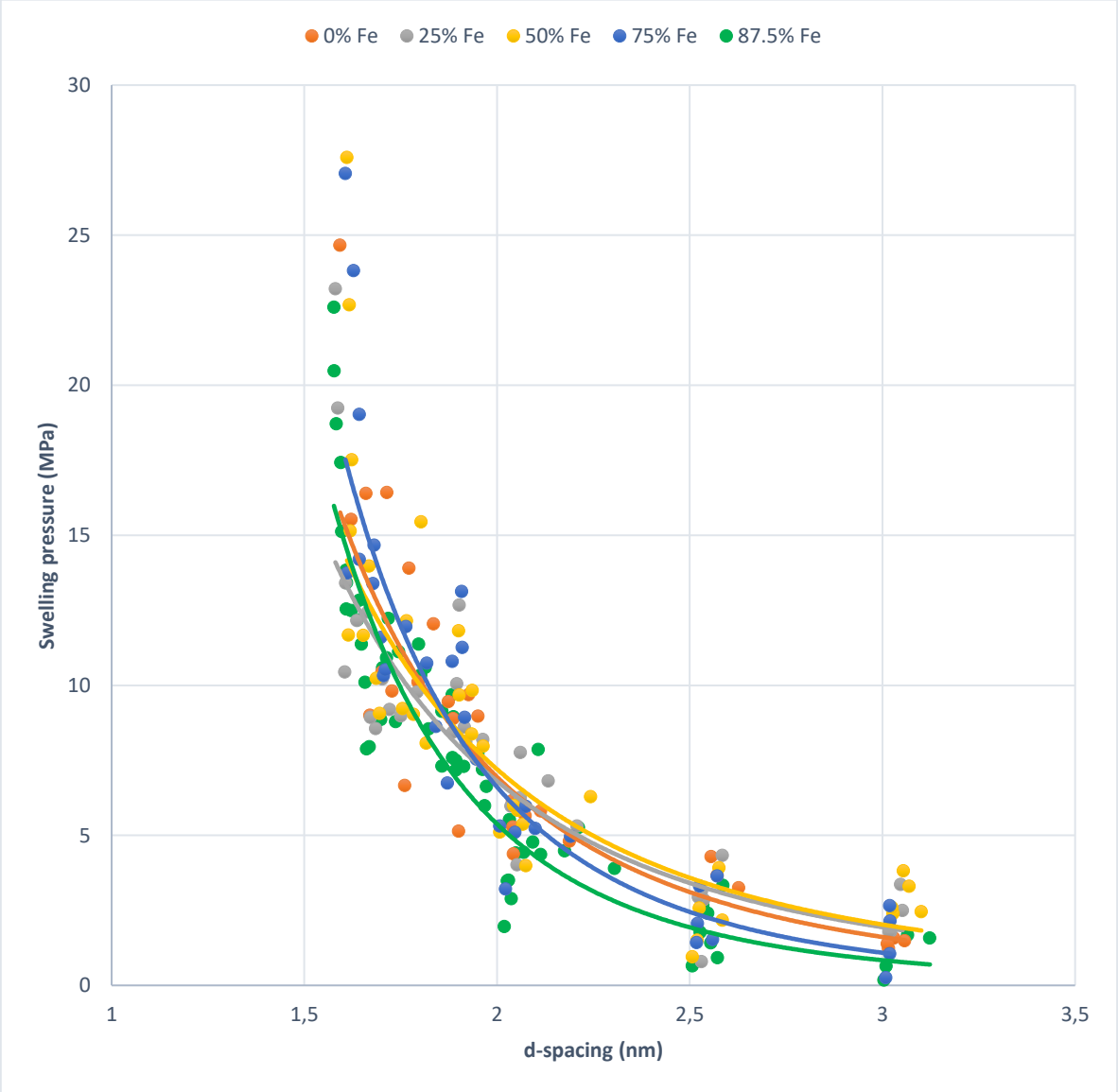

Figure 18(a). Comparison of samples of structure A with varying Fe-content

Table 3. Power and exponential fittings for Structure A

	POWER FIT		EXPONENTIAL FIT	
% Fe-CONTENT	FUNCTION	R^2	FUNCTION	R^2
0	$y = 84.246x^{-3,6}$	0.90	$y = 174.28e^{-1,581x}$	0.89
25	$y = 58.129x^{-3,094}$	0.78	$y = 112.21e^{-1,373x}$	0.77
50	$y = 62.834x^{-3,125}$	0.74	$y = 111.4e^{-1,342x}$	0.69
75	$y = 144.61x^{-4,451}$	0.82	$y = 374.99e^{-1,98x}$	0.81
87.5	$y = 128.71x^{-4,581}$	0.82	$y = 383.38e^{-2,093x}$	0.81

Table 4. Showing values for structure A at different Fe-content

D-spacing(nm)	Dry Density(kg/m^3)	Swelling Pressure, P(MPa)	ΔP(MPa)
	Structure A_0% $Si_{32}(Al_{14}Mg_2)O_{80}(OH)_{16}(OH_2)_8$		
1.6	1500	17.8	
2.0	1200	6.6	
2.7	900	2.5	
	Structure A_25% $Si_{32}(Al_{10}Fe_4Mg_2)O_{80}(OH)_{16}(OH_2)_8$		
1.7	1500	13.4	-4.4
2.1	1200	5.6	-1.0
2.8	900	2.3	-0.2
	Structure A_50% $Si_{32}(Al_6Fe_8Mg_2)O_{80}(OH)_{16}(OH_2)_8$		
1.7	1500	10.5	-7.3
2.2	1200	4.7	-1.9
2.9	900	2.1	-0.4
	Structure A_75% $Si_{32}(Al_2Fe_{12}Mg_2)O_{80}(OH)_{16}(OH_2)_8$		
1.8	1500	10.8	-7.0
2.2	1200	4.2	-2.4
3.0	900	1.7	-0.8
	Structure A_87.5% $Si_{32}(Fe_{14}Mg_2)O_{80}(OH)_{16}(OH_2)_8$		
1.8	1500	7.9	-9.9
2.3	1200	2.8	-3.8
3.0	900	1.0	-1.5

9.1.2 **Clay structure C - $(Si_{30}Al_2)(Al_{16})O_{80}(OH)_{16}(0H_2)_8$**

Structure C has -0.50 layer charge an 100% charge in the tetrahedral sheet. In structure C, significant swelling was observed, although the swelling pressure of structure C at different Fe-content is smaller compared to structure A. Figure 18(b) shows a decline in swelling pressure with increasing d-spacing as observed in structure A.

Table 5 compare the power and exponential function of the graph shown in Figure 18(b) and they are almost the same. As was observed in structure A, the fittings observed in structure C (as shown in Figure 18(b)) are very good as well. Little decrease in swelling pressure with increase in Fe-content was observed in structure C as shown in Table 6. Table 6 shows the d-spacings at 1500, 1200 and 900 kg/m^3 with their corresponding swelling pressures and change in swelling pressures (ΔP).

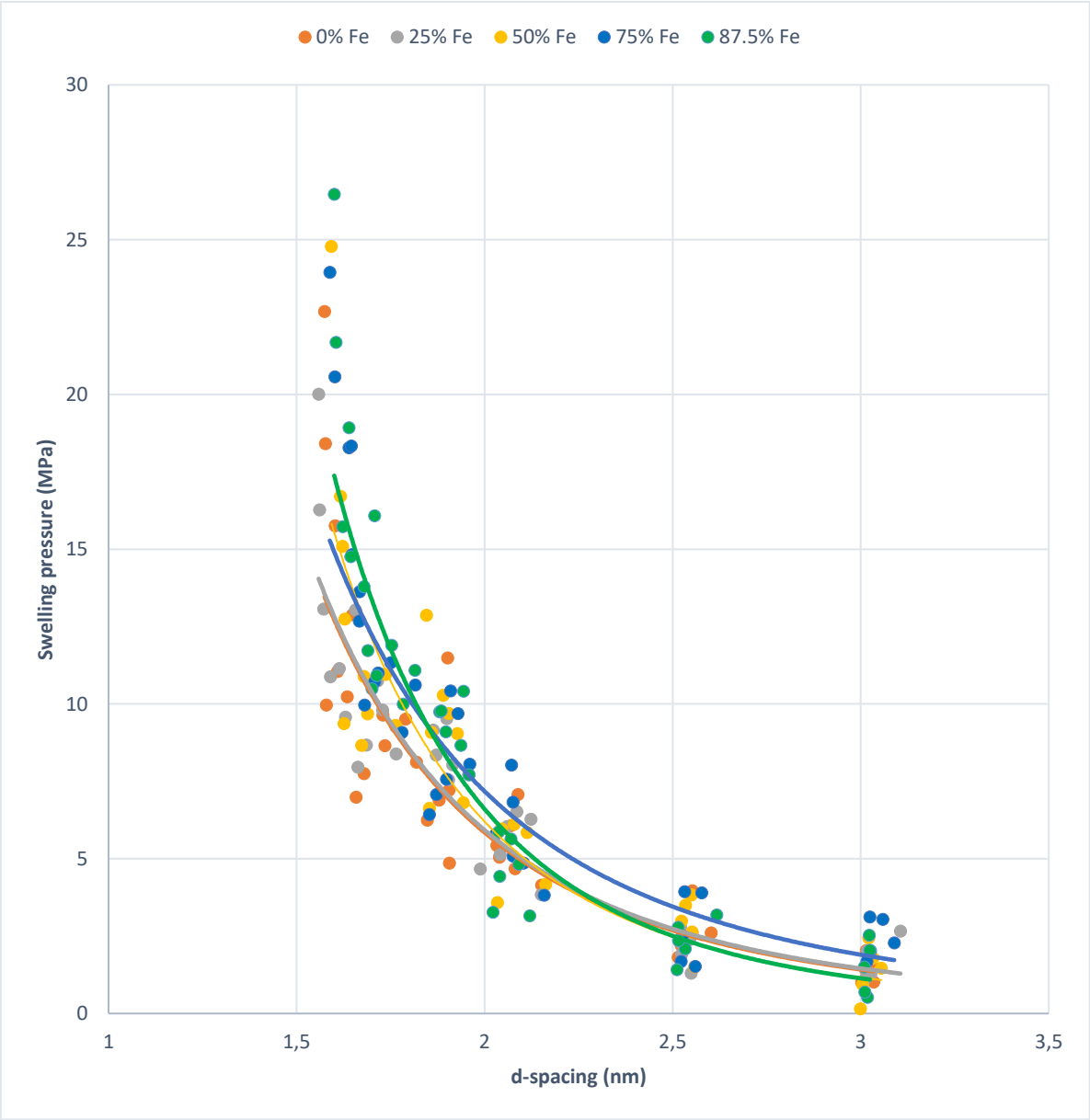

Figure 18(b). Comparison of samples of structure C with varying Fe-content

Table 5. Power and exponential fittings for Structure C

	POWER FIT		EXPONENTIAL FIT	
% Fe-CONTENT	FUNCTION	R^2	FUNCTION	R^2
0	$y = 65.409x^{-3,484}$	0.90	$y = 143.04e^{-1,562x}$	0.89
25	$y = 65.251x^{-3,461}$	0.90	$y = 139.12e^{-1,542x}$	0.88
50	$y = 107.62x^{-4,118}$	0.77	$y = 264.27e^{-1,838x}$	0.79
75	$y = 69.614x^{-3,278}$	0.85	$y = 130.36e^{-1,421x}$	0.81
87.5	$y = 133.42x^{-4,337}$	0.88	$y = 323.77e^{-1,908x}$	0.86

Table 6. Showing values for structure C at different Fe-content

D-spacing(nm)	Dry Density(kg/m^3)	Swelling Pressure, P(MPa)	ΔP(MPa)
	Structure C_0% $(Si_{30}Al_2)(Al_{16})O_{80}(OH)_{16}(OH_2)_8$		
1.6	1500	12.0	
2.0	1200	4.7	
2.7	900	1.9	
	Structure C_25% $(Si_{30}Al_2)(Al_{12}Fe_4)O_{80}(OH)_{16}(OH_2)_8$		
1.7	1500	11.8	-0.2
2.1	1200	4.5	-0.2
2.8	900	1.7	-0.2
	Structure C_50% $(Si_{30}Al_2)(Al_8Fe_8)O_{80}(OH)_{16}(OH_2)_8$		
1.7	1500	11.3	-0.7
2.2	1200	4.2	-0.5
2.9	900	1.6	-0.3
	Structure C_75% $(Si_{30}Al_2)(Al_4Fe_{12})O_{80}(OH)_{16}(OH_2)_8$		
1.8	1500	10.3	-1.7
2.2	1200	4.3	-0.4
3.0	900	1.8	-0.1
	Structure C_87.5% $(Si_{30}Al_2)(Al_2Fe_{14})O_{80}(OH)_{16}(OH_2)_8$		
1.8	1500	9.4	-2.6
2.3	1200	3.5	-1.2
3.0	900	1.3	-0.6

9.1.3 **Clay structure H - $Si_{32}(Al_{12}Mg_4)O_{80}(OH)_{16}(0H_2)_8$**

Structure H has -1.00 layer charge and 0% charge in the tetrahedral sheet. Maximum iron substitution achievable in structure H is 75%. Structure H shows a decreasing trend in the swelling pressure with increase in d-spacing as observed in structures A and C. This is shown in figure 18(c) with corresponding fittings in Table 7. Table 7 compares the power and exponential function of structure H as shown in Figure 18(c). The fittings are good except for the case with 50% Fe-content. Table 8 shows the little effect of increasing Fe-content on the swelling pressure of structure H, which is similar to what was observed in structure C.

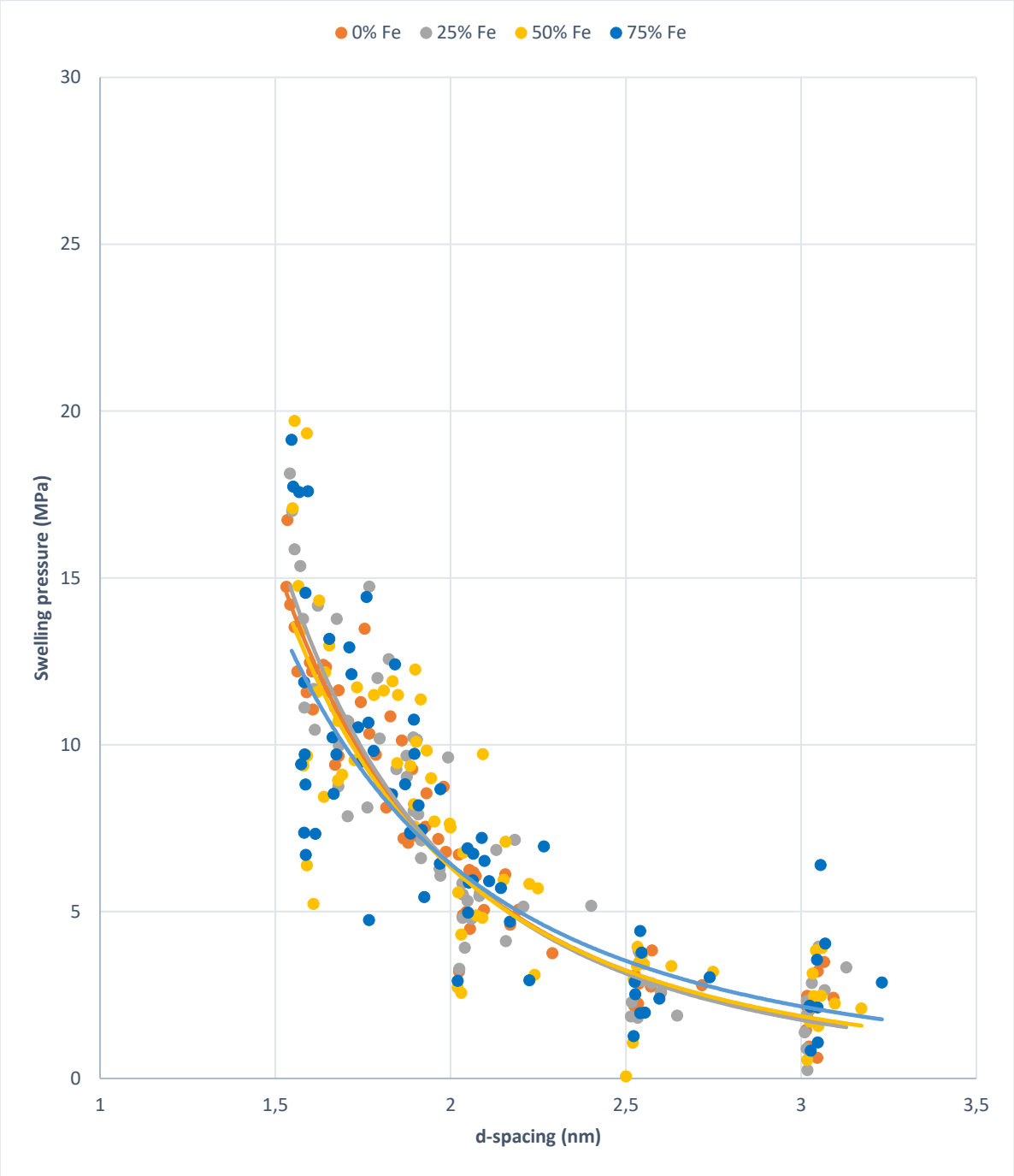

Figure 18(c). Comparison of samples of structure H with varying Fe-content

Table 7. Power and exponential fittings for Structure H

	POWER FIT		EXPONENTIAL FIT	
% Fe-CONTENT	FUNCTION	R^2	FUNCTION	R^2
0	$y = 53.878x^{-3,071}$	0.88	$y = 104.4e^{-1,365x}$	0.86
25	$y = 58.973x^{-3,199}$	0.77	$y = 117.04e^{-1,421x}$	0.76
50	$y = 50.898x^{-3,007}$	0.53	$y = 94.78e^{-1,324x}$	0.52
75	$y = 41.378x^{-2,687}$	0.71	$y = 72.919e^{-1,187x}$	0.69

Table 8. Showing values for structure H at different Fe-content

D-spacing(nm)	Dry Density(kg/m^3)	Swelling Pressure, P(MPa)	ΔP(MPa)
	Structure H_0% $Si_{32}(Al_{12}Mg_4)O_{80}(OH)_{16}(OH_2)_8$		
1.6	1500	12.8	
2.0	1200	5.7	
2.7	900	2.5	
	Structure H_25% $Si_{32}(Al_8Fe_4Mg_4)O_{80}(OH)_{16}(OH_2)_8$		
1.7	1500	11.1	-1.7
2.1	1200	4.9	-0.8
2.8	900	2.2	-0.3
	Structure H_50% $Si_{32}(Al_4Fe_8Mg_4)O_{80}(OH)_{16}(OH_2)_8$		
1.7	1500	9.8	-3.0
2.2	1200	4.6	-1.1
2.9	900	2.2	-0.3
	Structure H_75% $Si_{32}(Fe_{12}Mg_4)O_{80}(OH)_{16}(OH_2)_8$		
1.8	1500	7.9	-4.9
2.2	1200	4.2	-0.7
3.0	900	2.2	-0.3

9.1.4 **Clay structure J - $(Si_{28}Al_4)(Al_{16})O_{80}(OH)_{16}(0H_2)_8$**

Structure J has -1.00 layer charge and 100% charge in the tetrahedral sheet. Structure J also shows a decreasing trend in the swelling pressure with increase in d-spacing as was seen in structures A, C and H. This is shown in Figure 18(d). In clay structure J, lower swelling pressure was observed in samples with low Fe content (J_0% and J_25%), more swelling was observed in structures with higher Fe content (structures J_50%, J_75% and J_87.5%). Table 9 shows a comparison between power and exponential functions of the graph shown in Figure 18(d), in which case both functions are almost the same. The fittings obtained for structure J (as shown in Figure 18(d)) is not so good compared to the fittings obtained for structures A, C and H.

Decrease in the swelling pressure with increase in Fe-content is also prominent in structure J as was observed in structure A. This is shown in Table 10 which also shows the d-spacing values at 1500, 1200 and 900 kg/m^3 with their corresponding swelling pressures and change in swelling pressures (ΔP).

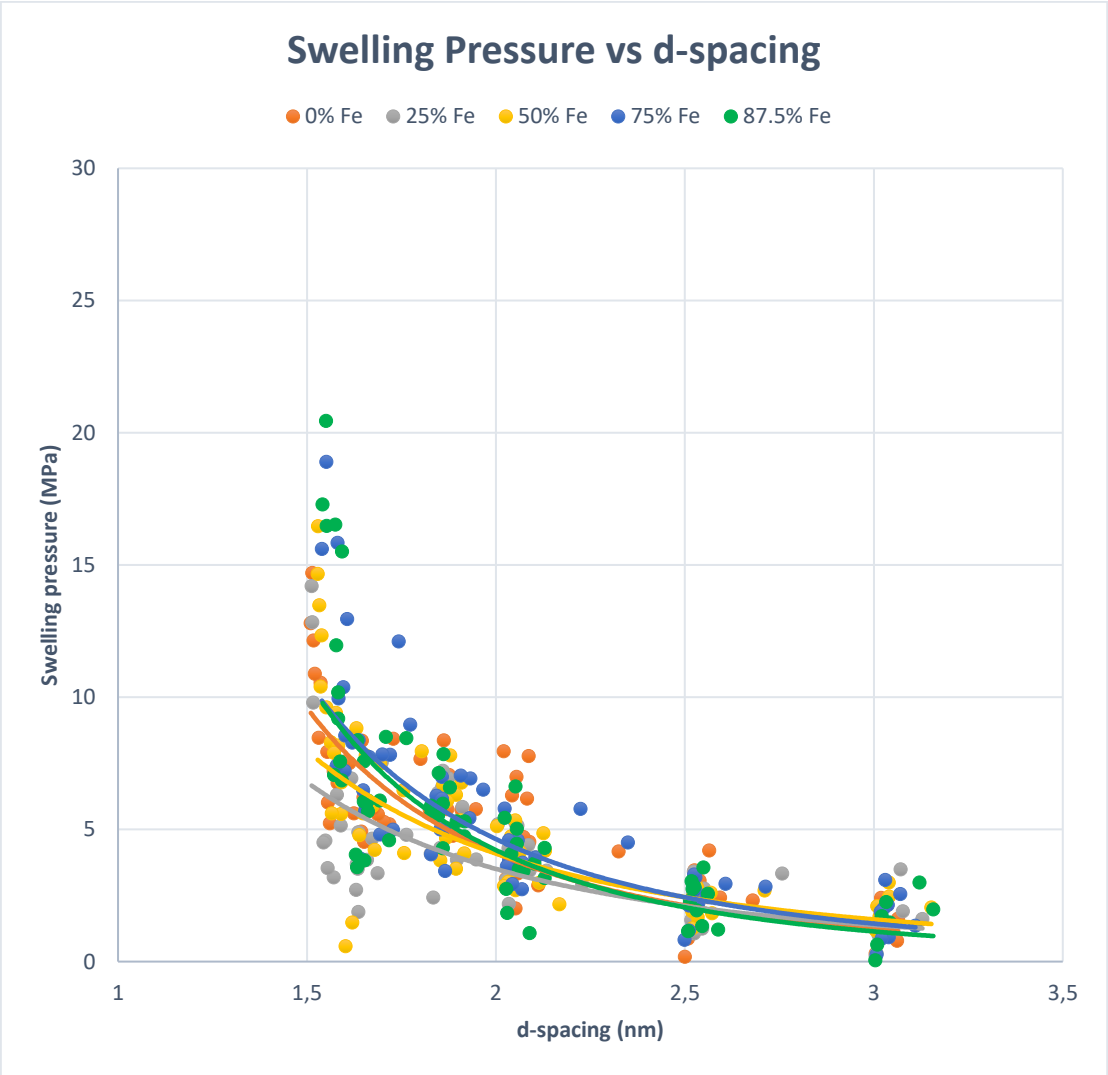

Figure 18(d). Comparison of samples of structure J with varying Fe-content

Table 9. Power and exponential fittings for Structure J

	POWER FIT		EXPONENTIAL FIT	
% Fe-CONTENT	FUNCTION	R^2	FUNCTION	R^2
0%	$y = 31.766x^{-2,953}$	0.64	$y = 66.35e^{-1,356x}$	0.64
25%	$y = 17.207x^{-2,296}$	0.52	$y = 30.37e^{-1,052x}$	0.53
50%	$y = 20.418x^{-2,321}$	0.57	$y = 34.645e^{-1,041x}$	0.55
75%	$y = 34.333x^{-2,889}$	0.70	$y = 64.251e^{-1,284x}$	0.69
87.5%	$y = 39.446x^{-3,226}$	0.59	$y = 80.844e^{-1,441x}$	0.58

Table 10. Showing values for structure J at different Fe-content

D-spacing(nm)	Dry Density(kg/m^3)	Swelling Pressure, P(MPa)	ΔP(MPa)
	Structure J_0% $(Si_{30}Al_2)(Al_{16})O_{80}(OH)_{16}(OH_2)_8$		
1.6	1500	7.6	
2.0	1200	3.6	
2.7	900	1.7	
	Structure J_25% $(Si_{30}Al_2)(Al_{16})O_{80}(OH)_{16}(OH_2)_8$		
1.7	1500	5.3	-2.3
2.1	1200	3.0	-0.6
2.8	900	1.7	0
	Structure J_50% $(Si_{28}Al_4)(Al_8Fe_8)O_{80}(OH)_{16}(OH_2)_8$		
1.7	1500	5.7	-1.9
2.2	1200	3.2	-0.4
2.9	900	1.8	0.1
	Structure J_75% $(Si_{28}Al_4)(Al_4Fe_{12})O_{80}(OH)_{16}(OH_2)_8$		
1.8	1500	6.1	-1.5
2.2	1200	3.1	-0.5
3.0	900	1.5	-0.2
	Structure J_87.5% $(Si_{28}Al_4)(Al_2Fe_{14})O_{80}(OH)_{16}(OH_2)_8$		
1.8	1500	5.3	-2.3
2.3	1200	2.5	-1.1
3.0	900	1.2	-0.5

9.2 **Dry density versus d-spacing**

Swelling pressure of all structures without Fe and with varying percentage of Fe-content was calculated from their dry densities. Dry density is a function of the weight of the iron atom and this has more effect than d-spacing. Dry densities of clay samples studied were calculated using the formula below.

$$\text{Dry density} = \frac{mass\ of\ clay}{volume\ of\ clay} = \frac{mass\ of\ clay}{(clay\ surface\ area * d{-}spacing)}$$

Increment in the Fe-content in all studied structures causes increase in the dry density values. At fixed dry density values, d-spacing increases with increase in Fe-content. The increasing trend in d-spacings with increase in Fe-content of each studied structure at 1500kg/m^3, 1200kg/m^3 and 900kg/m^3 dry density values is shown in Tables 11, 12 and 13 respectively. The most effect is observed at 900kg/m^3 dry density value.

Table 11. Comparison of d-spacings of studied structures at varying Fe-content percentage at 1500 kg/m^3

	D-SPACING (nm) AT 1500 kg/m^3				
STRUCTURE	0% Fe	25% Fe	50% Fe	75% Fe	87.5% Fe
A	1.609	1.671	1.732	1.794	1.825
C	1.611	1.673	1.734	1.796	1.826
H	1.607	1.688	1.730	1.791	-
J	1.610	1.671	1.733	1.794	1.825

Table 12. Comparison of d-spacings of studied structures at varying Fe-content percentage at 1200 kg/m^3

	D-SPACING (nm) AT 1200 kg/m^3				
STRUCTURE	0% Fe	25% Fe	50% Fe	75% Fe	87.5% Fe
A	2.012	2.089	2.165	2.242	2.281
C	2.014	2.091	2.168	2.244	2.283
H	2.008	2.085	2.162	2.239	-
J	2.012	2.089	2.166	2.243	2.281

Table 13. Comparison of d-spacings of studied structures at varying Fe-content percentage at 900 kg/m^3

	D-SPACING (nm) AT 900 kg/m^3				
STRUCTURE	0% Fe	25% Fe	50% Fe	75% Fe	87.5% Fe
A	2.682	2.785	2.887	2.990	3.041
C	2.685	2.788	2.890	2.993	3.044
H	2.678	2.780	2.883	2.985	-
J	2.683	2.786	2.888	2.991	3.042

The higher the dry density values of clay samples, the higher the swelling pressures of such clay samples. However, at a fixed dry density value, increase in Fe-content of clay samples leads to a decrease in their swelling pressures. This trend is shown in Tables 14-16. Tables 14, 15 and 16 show the swelling pressure values of all studied samples at dry density values 1500, 1200 and 900 kg/m^3 respectively.

Table 14. Comparison of swelling pressures of studied structures with varying Fe-content percentage at 1500 kg/m^3

	SWELLING PRESSURE (MPa) AT 1500 kg/m^3				
STRUCTURE	0% Fe	25% Fe	50% Fe	75% Fe	87.5% Fe
A	17.8	13.4	10.5	10.8	7.9
C	12.0	11.8	11.3	10.3	9.4
H	12.8	11.1	9.8	7.9	-
J	7.6	5.3	5.7	6.1	5.3

Figure 19 shows the behavior of swelling pressure of structures A, C, J and H with increasing Fe-content at 1500 kg/m^3 dry density as presented in Table 14. Increase in Fe-content of each clay sample causes a reduction in the swelling pressure. The most effect of Fe-content on the swelling pressure of clay samples is seen at about 25% as shown in Figure 19. Effect of iron on the swelling pressures of clay samples is more prominent in structures A and H (montmorillonite clay samples) when compared to structures C and J (beidellite clay samples).

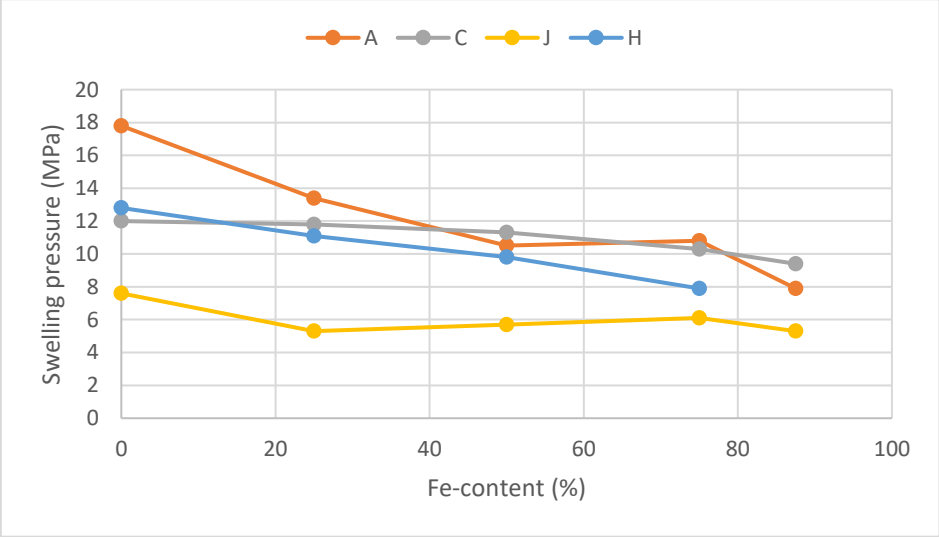

Figure 19. Swelling pressure behavior with increase in Fe-content

Table 15. Comparison of swelling pressures of studied structures at varying Fe-content percentage at 1200 kg/m^3

	SWELLING PRESSURE (MPa) AT 1200 kg/m^3				
STRUCTURE	0% Fe	25% Fe	50% Fe	75% Fe	87.5% Fe
A	6.6	5.6	4.7	4.2	2.8
C	4.7	4.5	4.2	4.3	3.5
H	5.7	4.9	4.6	4.2	-
J	3.6	3.0	3.2	3.1	2.5

Figure 20 shows the behavior of swelling pressure of structures A, C, J and H with increasing Fe-content at 1200 kg/m^3 dry density as shown in Table 15. The swelling pressures drop as the Fe-content of each clay sample increases. Although a bit less but similar to the case at 1500kg/m^3 dry density, the effect of iron is more obvious on the montmorillonite clay samples (structures A and H) than on the beidellite clay sample (structures C and J) at 1200 kg/m^3 dry density.

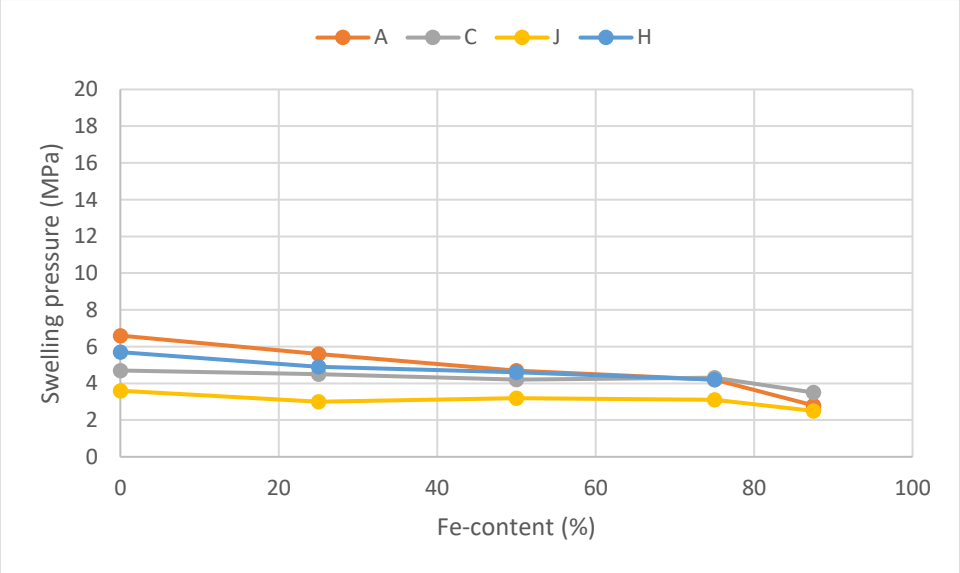

Figure 20. Swelling pressure behavior with increase in Fe-content

Table 16. Comparison of swelling pressures of studied structures at varying Fe-content percentage at 900 kg/m^3

	SWELLING PRESSURE (MPa) AT 900 kg/m^3				
STRUCTURE	0% Fe	25% Fe	50% Fe	75% Fe	87.5% Fe
A	2.5	2.3	2.1	1.7	1.0
C	1.9	1.7	1.6	1.8	1.3
H	2.5	2.2	2.2	2.2	-
J	1.7	1.7	1.8	1.5	1.2

Figure 21 shows the behavior of swelling pressure of structures A, C, J and H with increasing Fe-content at 900 kg/m^3 dry density as presented in Table 16. At this dry density value, all structures have almost the same behavior. Very little effect of iron is observed on the swelling pressures of all studied structures. As is shown in Figure 21 below, increase in Fe-content for all clay samples has very little effect on their swelling pressures.

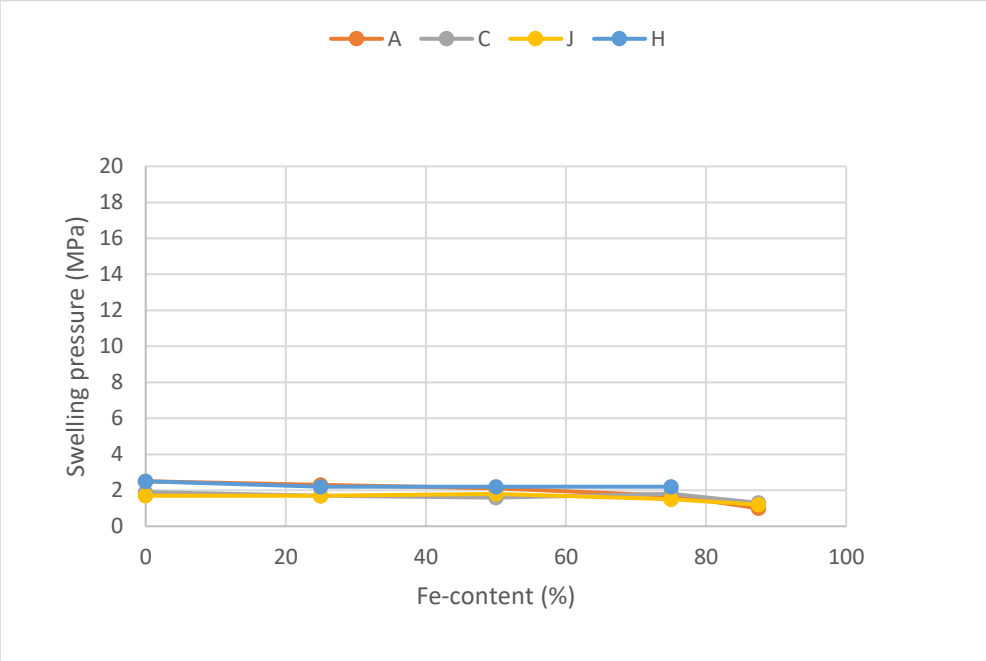

Figure 21. Swelling pressure behavior with increase in Fe-content

The amount of iron observed in clay samples is typically below 25%. In general, the effect of iron on the swelling pressure of all structures studied is small. The effect of Fe-content on the swelling pressure of clay samples is more prominent in structures A and J (montmorillonite clay samples) than in structures C and H (beidellite clay samples) at high dry density.

CHAPTER 10: CONCLUSIONS AND OUTLOOK

Presently, little experimental studies are available on the effect of iron on the swelling pressure of smectites. According to study by Stucki (1988) [56] increase in Fe-content leads to reduction in the swelling pressure of the clay. This is evident in this study as shown in figures 19-21. It was observed that the effect of iron on the swelling pressure of all studied structures is not much but the little effect is more pronounced in structures A and H than structures C and J.

Effect of Fe-content on swelling pressures is more prominent in montmorillonite clay samples (structures A and H) than beidellite clay samples (structures C and J). This finding is important in the choice of smectites as engineering barriers. The model used was effective and the result obtained gave a trend which is in good agreement with previous studies on the effect of iron on the swelling pressures of smectites.

Computational studies on the effect of insitu reduction of Fe^{3+} to Fe^{2+} on swelling pressure of smectites is an area of interest. I have an interest in exploring what happens to the swelling abilities of expansive clay materials if Fe^{3+} reduces to Fe^{2+} because of the unstable nature of Fe.

ACKNOWLEDGEMENT

I appreciate the effort and unflinching support of my supervisors, Linlin Sun, Janne Hirvi and Tapani Pakkanen. I acknowledge the grants of computer capacity from the Finnish Grid and Cloud Infrastructure (persistent identifier urn:nbn:fi:research-infras-2016072533), and I am also grateful to everyone who in various ways have offered their support. Finally, my deep gratitude to God Almighty who made His grace sufficient for me.

REFERENCES

1. Howard, A.B., Thixotropy-A Review, J. of Non-newtonian Fluid Mech., 1997 (70), 7
2. Guggenheim Stephen, Introduction to the Properties of Clay Minerals, In Teaching Mineralogy, Brady, J.B.,Mogt, D.W., and Perkins, D. III, (Eds.), Mineralogical Society of America, Washington, D.C , 1997, 371-388.
3. Mockovciakova, A.; Orolinova Z., Adsorption Properties of Modified Bentonite Clay, Chem. Technol. 2009 (1) 47-50
4. Barton, C.D, Karanthanasis, A.D, Encyclopedia of Soil Science, 2002
5. Dr. Thair Al-Ani and Dr. Olli Sarapää, Clay and Clay Mineralogy, Physical-chemical Properties and Industrial Uses, Geologian Tutkimuskeskus, 2008, 9, 10, 12, 17
6. Maio, Caterina Di, Swelling Pressure of Clayey Soils: The Influence of Stress State and Pore Liquid Composition, Rivista Italiana di Geotecnica, 2001 (3), 22
7. Teich-McGoldrick, S.L., Greathouse, J.A., Jove-Colon, C.F., Cygan, R.T., Swelling Properties of Montmorillonite and Beidellite Clay Minerals from Molecular Simulation: Comparison of Temperature, Interlayer Cation and Charge Location Effects, J. Phys. Chem. C 2015 (119), 20880-20891
8. Handbook of Clay Science, Second Edition, Part A: Fundamentals, edited by F. Bergaya and G. Lagaly, 2013, 22, 23, 25
9. Pinnavaia, T.J., Intercalated Clay Catalysts, Science, 1983 (220), 365-371; Laszlo, P., Catalysis of Organic Reactions by Inorganic Solids, Acc. Chem. Res., 1986(19), 121-127
10. Bruce Velde and Alain Meunier, The Origin of Clay Minerals in Soils and Weathered Rocks, 2008, 4
11. Janek, M., komadel, P., Lagaly G., Effect of Autotransformation on the Layer Charge of Smectites Determined by the Alkylammonium Method, Clay Miner., 1997(32), 623-632
12. Schulze, D.G, Clay Minerals, Purdue University, West Lafayette, IN, USA, Elsevier Ltd., 2005, 246-254
13. Lagaly, G., Layer Charge Determination by Alkylammonium ions. Layer Charge Characteristics of 2:1 Silicate Clay Minerals, 1994

14. Osthaus, B.B., Chemical Determination of Tetrahedral Ions in Nontronite and Montmorillonite, 1954, 404-417. In Ada Swineford and Norman Plummer (eds.), Clays and Clay Minerals, Proc. 2nd Natl. Conf., Columbia, Missouri, 1953, Natl. Acad. Sci. Natl. Res. Counc. Publ., 327, Washington, D.C
15. Grim, R.E., Clay Mineralogy, McGraw-Hill, Inc., New York, 596
16. Tom Schanz and Snehasis Tripathy, Swelling Pressure of a Divalent-Rich Bentonite: Diffuse Double-Layer Theory Revisited, Water Resources Research, 2009(45), 1-9
17. Antti Lempinen, Mechanical Stability of Bentonite Buffer System for High level Nuclear Waste, 1998, 10
18. Jinsong Liu and Ivars Neretnieks, Physical and Chemical Stability of the Bentonite Buffer, 2006, 9,11,12
19. Patricia Shapley, Clay Minerals Lecture Note, Department of Chemistry,University of Illinois, 2010
20. Vulliet, L., Laloui, L., Harding, R., Environmental Geomachanics: An Introduction. In Environmental Geomechanics, Vulliet, L., Laloui, L., Schrefler, B. (eds.). EPFL-Press: Lausanne, 2002, 3-12
21. Marshall, C.E, The Colloid Chemistry of the Silicate Mineral, New York: Academic Press, 1949
22. Donna, R., Bentonite Clay Adsorbs Radiation, NaturalNews.com, 2011
23. Nandi, B.K., Goswami, A., Purkait, M.K., Adsorption Characteristics of Brilliant Green dye on Kaolin, J. Hazard. Mater., 2009, 161 (1), 387-395
24. Barshad, I., Adsorptive and Swelling Properties of Clay-water System, Clays and Clay Minerals, 1952(1), 70-77
25. Dohrmann, R., Cation Ion Exchange Capacity Methodology III: Correct Exchangeable Calcium Determination of Calcareous Clays Using a new Silver-Thiourea Method, Appl. Clay Sci., 2006 (34), 47-57
26. Robert, H.S. Robertson, Clay Minerals as Catalysts, 49
27. American Geological Institute, 1972. Glossary of Geology Pub. American Geological Institute
28. Daniel, D., Earthen Liners for Land Disposal Facilities. In Geotechnical Practice for Waste Disposal ’87, GSP No. 13, ASCE, 1987, 21-39
29. Gartell, J.E. et al., Arlington, VA: National Science Teachers Association, 1992
30. Reed J.S., Principles of Ceramic Processing, 2nd ed. New York: Wiley; 1995
31. Breen, C., Zahoor, F., Madejova, D., Komadel, P.J., Characterization and catalytic activity of Acid Treated, Size Fractionated Smectites, J. Phys. Chem., B, 1997 (101), 5324-5331
32. Lussier, R.J., A Novel Clay Based Catalytic Material- Preapration and Properties, J. Catal., 1991 (129), 225-237
33. Narayanan, S., Deshpande, K., Synthetic Mica Montmorillonite and Wyoming Montmorillonite: Effect of acid Activation on Structural and Catalytic Properties, Recent Trends Catal. 1999, 344-352
34. Sabu, K.R., Lalithambika, M., Acidic Properties and Catalytic Activity of Natural Kaolinite Clays for Friedel-Crafts Alkylation, Bull. Chem. Soc. Jpn., 1993 (66), 3535-3541

35. Narayanan, S., Deshpande, K., Alumina Pillared Montmorillonite: Characterization and Catalysis of the Toluene Benzylation and Aniline Ethylation, Appl. Catal. A gen., 2000 (193), 17-27
36. Howard, A.B., Thixotropy-A Review, J. of Non-newtonian Fluid Mech., 1997 (70), 7
37. Mitchell, J.K., Fundamentals of Soil Behavior, John Wiley, 1993
38. Kaufhold, S., Baille, W., Schanz, T., Dorhmann, R., About Differences of Swelling Pressure- dry Density Relations of Compacted Bentonites, Applied Clay Science 2015 (107), 52-61
39. Komine, H., Simplified Evaluation for Swelling Characteristics of Bentonites, Engineering Geology,2004 (71), 265-279
40. Wayllace, A., Volume Change and Swelling Pressure of Expansive Clay in the Crystalline Swelling Regime, Ph.D. Thesis, University of Missouri, 2008, 2
41. Cornet, I., Expansion of the Montmorillonite Lattice on Hydration, J. Chemical Physics, 1950 (18), 623-626
42. Mooney, R.W., Keenan, A.G., Wood, L.A, Adsorption of Water Vapor by Montmorillonite. II. Effect of Exchangeable Ions and Lattice Swelling as Measured by X-ray Diffraction, J. Am. Chem. Soc. 1952 (74), 1371-1374
43. Morodome, S., Kawamura, K., Swelling Behavior of Na and Ca-Montmorillonite up to 150^0C by in situ X-ray Diffraction Experiments, clays Clay Miner. 2009 (57) , 150-160
44. Bolt, G.H., Physico-Chemical Analysis of the Compressibility of Pure Clays, Geotechnique, 1956, vol. VI, n. 1, 86-93
45. Abduljauwad, S.N., Al-Sulaimani, G.J., Badunsbul, I.A., Al-Buraim I., laboratory and Field Studies of Response of Structures to Heave of Expansive Clay, Geo-technique, vol. XLVIII, n. 1, 103-121
46. Wilson, M.J., Soil Smectites and Related Interstratified Minerals: Recent Developments, 1987, 167-173. In Schulze, L.G., Van Olphen, H., and F.A. Mumpton (eds.), Proc. Int. Clay Conf., Denver, 1985, The Clay Minerals Society, Bloomington, Indiana
47. Nahon, D., Collin, F. and Tardy, Y., Formation and Distribution of Mg, Fe, Mn-Smectites in the First Stages of the Lateritic Weathering of Forsterite and Tephroite, Clay Miner., 1982 (17), 339-348
48. Seyfried, W. R., Jr., and Bischoff, J.L., Low Temperature basalt Alterartion by Seawater: An Experimental Study at 70 Degree C and 150 Degree C, Geochim. Cosmochim. Acta, 1979 (43), 1937-1947
49. Isphording, W.C., Primary Nontronite from Venezuelan Guyana, Am. Mineral, 1975 (60), 840-848
50. NASA/JPL- Caltech/University of Arizona/Imperial College London
51. Brindley, G.W., Order-Disorder in Clay Mineral Structures. In: Brindley, G.W.,Brown, G. (Eds.), Crystal Structures of Clay Minerals and their X-ray Identification, Mineralogical Society, London, 125-195
52. Brigatti, M,F., Relationships Between Composition and Structure in Fe-rich Smectites, Clay Miner., 1983 (18), 177-186
53. Charpentier, D., Buatier, M.D., Jacquot, E., Gaudin, A., Wheat, C.G., Conditions and Mechanism for the Formation of Iron-rich Montmorillonite in Deep sea Sediments

(Costa Rica Margin): Coupling High Resolution Mineralogical Characterization and Geochemical Modelling, Geochimica et Cosmochimica Acta, 2011 (75), 1397-1410
54. Charadi, K., Gondran, C., Be Haj Amara, A., Prevot, V., Mousty, C., H2O2 Determination at Iron-rich Clay Modified Electrodes, Electrochemica Acta, 2009 (54), 4237-4244
55. Earth Sciences Museum/University of Waterloo
56. Stucki, J.W., Structural Iron in Smectites, Iron in Soils and Clay Minerals, 1988, 625-675
57. Marfunin A.s., Mkrtchyan, A.R., Nadzharyan, G.N., Nyussik, Y.M. and Platonov, A.N., Optical and Mossbauer Spectra of Iron in some Layered Silicates, 1971, Izv. Akad. Nauk. SSSR, Ser. Geol. 1971, 87-93
58. Roth, C.B., Jackson, M. L., Lotse, E.G. and syers, J.K., Ferrous-ferric Ratio and C.E.C changes on Deferration Weathered Micaceous Vermiculites, Isr. J. Chem., 1968 (6), 261-273
59. Roth, C.B., Jackson, M. L., and syers, J.K., Deferration Effect on Structural Ferrous-ferric Iron Ratio and CEC of Vermiculites and Soils, Clays Clay Miner., 1969 (17), 253-264
60. Stucki, J.W. and Roth, C.B., Oxidation-reduction Mechanism for Structural for Structural Iron in Nontronite, Soil Sci. Soc. Am. J., 1977 (41), 808-814
61. Stucki, J.W., Golden, D.C., and Roth, C.B., Effect of Reduction and Reoxidation of Structural Iron on the Surface Charge and Dissolution of Dioctahedral Smectites, Clays Clay Miner., 1984b (32), 350-356
62. Harder, H., Synthesis of Iron Layer Silicate Minerals Under Natural Conditions, Clays Clay Miner., 1978 (26), 65-72
63. Stucki, J.W., Komadel, P. and Wilkinson, H.T., The Microbial Reduction of Structural Iron (III) in Smectites, 1987, Soil Sci. Soc. Am. J.
64. Chen, Y., Shaked, D. and Banin, A., The Role of Structural Iron (III) in the UV Absorption by Smectites, Clay Miner., 1979 (14), 93-102
65. Roth, C.B. and Tullock, R.J, Deprotonation of Nontronite resulting from Chemical Reduction of Structural Ferric Iron, 1973, 107-114. In Serratosa, J.M., (ed.) Proc. Int. Clay Conf., Madrid, 1972. Div. Ciencias C.S.I.C., Madrid
66. Anderson, R.L., Ratcliffe, I., Greenwell, H.C., Williams, P.A.,Cliffe, S., Coveney, P.V., Clay Swelling – A Challenge in the Oilfield, Earth-Science Reviews, 2010 (98), 201-216
67. Mering, J., On the Hydration of Montmorillonite. Transactions of the Faraday Society, 1946 (42B), 205-219
68. Diaz-Perez, A., Cortes-Monroy, I., Roegiers, J.C., The Role of Water/Clay Interaction in the Shale Characterization, Journal of Petroleum Science and Engineering, 2007 (58), 83-98
69. Guggenheim, S., Koster Van Groos, A.F., Baseline Studies of the Clay Minerals Society Source Clays: Thermal Analysis, Clays and Clay Minerals, 2001 (49), 433-443
70. Tuller, M., Or, D., Clays, Clay Minerals and Soil Shrink/Swell Behavior, 2002-2004, 75-100
71. Číčel,B. and Komadel P., Structural Formulae of Layer Silicates, Soil Sci. Soc. Am., 1994 (69), 114-136

72. Schatz, T., Martikainen, J., Laboratory Studies on the Effect of Freezing and Thawing Exposure on Bentonite Buffer Performance: Closed-System Tests, Posiva 2010-06, ISBN 978-951-652-177-3, ISSN 1239-3096, 2010, 11-12
73. Alonso, E.E., Ledesma, A., Advances in Understanding Engineered Clay Barriers, A.A. Balkema Publishers, ISBN 04-1536-544-9, 2005, 310
74. Dove, M.T., An Introduction to Atomistic Simulation Methods, Seminarios de la SEM, Vol 4, 7-37
75. Friesner, R.A., Ab initio Quantum Chemistry: Methodology and Applications, 2005, PNAS, Vol. 102, no. 19, 6648-6653
76. Hohenberg, P., Kohn, W., Phys. Rev. 1964 (1326), B864-B871
77. Martin, J.M.L., de Oliveria, G., J. Chem. Phys., 1999 (111), 1843-1856
78. Milman, V., Winkler, B., White, J.A., Pickard, C.J., Payne, M.C.,Akhmatskaya, E.V., Nobes, R.H., Int. J. Quantum Chem. 2000 (77), 895-910
79. Rohlfing, M., Louie, S.G., Phys. Rev., 2000 (B62), 4927-4944
80. Binder, K., Heermann, D.W., Monte Carlo Simulation in Statistical Physics, 2002, 4th Edition, Springer
81. Skipper, N.T., Refson, K., McConnell, J.D.C., Computer Simulation of Interlayer Water in 2:1 Clays, J. Chem. Phys. 1991b (94), 7434-7445
82. Greathouse, J.A., Refson, K., Sposito, G., Molecular Dynamics Simulation of Water Mobility in Magnesium-Smectite Hydrates, J. Am. Chem. Soc., 2000 (122), 11459-11464
83. Seppala, A., Puhakka, E., Olin, M., Effect of Layer Charge on Crystalline Swelling of Na+, K+ and Ca2+ Montmorillonites: DFT and Molecular Dynamics Studies, Clay Minerals, 2016 (51), 197-211
84. Berendsen, H.J.C., Postma, J.P.M., van Gunsteren, W.F., Hermans, J., Interaction Models for Water in Relation to Protein Hydration, 1981, 331-342. In: Intermolecular Forces (B. Pullman, editor), D. Reidel Publishing, Dordrecht, The Netherlands
85. Alexandrov, V., Rosso, K.M., Insights into the Mechanism of Fe (II) Adsorption and Oxidation at Fe-Clay Mineral Surfaces from First-Principles Calculations, J. Phys. Chem., 2013(117), 22880-22886
86. Alexandrov, V., Neumann, A., Scherer, M.M., Rosso, K.M., Electron Exchange and Conduction in Nontronite from First-Principles, J. Phys. Chem. C, 2013, 117(5), 2032-2040
87. Geatches, D.L., Clark, S.J., Greenwell, H.C., Iron Reduction in Nontronite-type Clay Minerals: Modelling a Complex System, Geochimica et Cosmochimica Acta, 2012(81), 13-27
88. Sun et al., Influence of Layer Charge and Charge Location on the Swelling Pressure of Dioctahedral Smectites, J. Chem. Phys., 2016 (473), 40-45
89. Sun et al., Estimation of Montmorillonite Swelling Pressure: A Molecular Dynamics Approach, J. Phys. Chem. C, 2015, 119(34), 19863-19868